Elsevier Editorial System(tm) for Plant Science

Manuscript Draft

Manuscript Number: PSL-D-16-00191R1

Title: Impact of anatomical traits of maize (Zea mays L.) leaf as affected by nitrogen supply and leaf age on bundle sheath conductance

Article Type: Research Paper

Keywords: microstructure, nitrogen content, diffusive resistance, C4 photosynthesis, image analysis

Corresponding Author: Mr. Moges Retta,

Corresponding Author's Institution:

First Author: Moges Retta

Order of Authors: Moges Retta; Xinyou Yin; Peter E.L van der Putten; Dennis Cantre; Herman N.C. Berghuijs; Quang Tri Ho; Pieter Verboven; Paul C Struik; Bart M Nicolai

Abstract: The mechanism of photosynthesis in C4 crops depends on the archetypal Kranz-anatomy. To examine how the leaf anatomy, as altered by nitrogen supply and leaf age, affects the bundle sheath conductance (gbs), maize (Zea mays L.) plants were grown under three contrasting nitrogen levels. Combined gas exchange and chlorophyll fluorescence measurements were done on fully grown leaves at two leaf ages. The measured data were analysed using a biochemical model of C4 photosynthesis to estimate gbs. The leaf microstructure and ultrastructure were quantified using images obtained from micro-computed tomography and microscopy. There was a strong positive correlation between gbs and leaf nitrogen content (LNC) while old leaves had lower gbs than young leaves. Leaf thickness, bundle sheath cell wall thickness and surface area of bundle sheath cells per unit leaf area (Sb) correlated well with gbs although they were not significantly affected by LNC. As a result, the increase of gbs with LNC was little explained by the alteration of leaf anatomy. In contrast, the combined effect of LNC and leaf age on Sb was responsible for differences in gbs between young leaves and old leaves. Future investigations should consider changes at the level of plasmodesmata and membranes along the CO2 leakage pathway to unravel LNC and age effects further.

Bart M. Nicolaï
Flanders Center of Postharvest Technology

Katholieke Universiteit Leuven,

Willem de Croylaan 42,

B-3001, Leuven, Belgium

06/14/2016

Dear Dr. Blumwald,

We wish to submit a revised version of the manuscript entitled "Impact of anatomical traits of maize (Zea mays L.) leaf as affected by nitrogen supply and leaf age on bundle sheath conductance" for consideration by the journal, Plant Science.

The comments and suggestions from the reviewers were very useful. Consequently, we have substantially improved the manuscript both in formatting and content. The changes in the manuscript have been highlighted in red color. In addition, we have prepared and included detailed responses to comments from the reviewers.

The objective and main story of this revised paper remain unchanged. We report on an investigation of the causal relationship between variations of bundle sheath conductance and leaf anatomy of young and old maize leaves each having three contrasting leaf nitrogen contents. We found a positive and significant scaling of bundle sheath conductance with leaf nitrogen content while also confirming their relationship. This relationship was less due to changes in leaf anatomy by leaf nitrogen content alone. In contrast, the impact of leaf nitrogen content in interaction with leaf age on leaf anatomy accounted for the variation of bundle sheath conductance. The paper should be of interest to readers in the areas of C_4 photosynthesis and leaf anatomy.

We confirm that this work is original and has not been published elsewhere nor is it currently under consideration for publication elsewhere. The authors do not have any conflict of interest.

Thank you for your consideration of this manuscript.

Sincerely,

Bart M. Nicolaï

Impact of anatomical traits of maize (*Zea mays* L.) leaf as affected by nitrogen supply and leaf age on bundle sheath conductance

Moges Retta[1,2], Xinyou Yin[2,3], Peter E.L. van der Putten[2,3], Cantre D[1], Herman N.C. Berghuijs[1,2,3], Quang Tri Ho[1], Pieter Verboven[1], Paul C. Struik[2,3], Bart M. Nicolaï[1]

[1] BIOSYST-MeBioS, KU Leuven / Flanders Center of Postharvest Technology, Willem de Croylaan 42, B-3001, Leuven, Belgium

[2] Centre for Crop Systems Analysis, Wageningen University, P.O. Box 430, 6700 AK Wageningen, The Netherlands

[3] BioSolar Cells, P.O. Box 98, 6700 AB Wageningen, The Netherlands

Corresponding author:

Bart M. Nicolaï, Flanders Center of Postharvest Technology / BIOSYST-MeBioS, KU Leuven, Willem de Croylaan 42, B-3001 Leuven, Belgium

Email: bart.nicolai@biw.kuleuven.be

Tel: +32 16 322375

Fax: +32 16 322955

Abstract

The mechanism of photosynthesis in C_4 crops depends on the archetypal Kranz-anatomy. To examine how the leaf anatomy, as altered by nitrogen supply and leaf age, affects the bundle sheath conductance (g_{bs}), maize (*Zea mays* L.) plants were grown under three contrasting nitrogen levels. Combined gas exchange and chlorophyll fluorescence measurements were done on fully grown leaves at two leaf ages. The measured data were analysed using a biochemical model of C_4 photosynthesis to estimate g_{bs}. The leaf microstructure and ultrastructure were quantified using images obtained from micro-computed tomography and microscopy. There was a strong positive correlation between g_{bs} and leaf nitrogen content (LNC) while old leaves had lower g_{bs} than young leaves. Leaf thickness, bundle sheath cell wall thickness and surface area of bundle sheath cells per unit leaf area (S_b) correlated well with g_{bs} although they were not significantly affected by LNC. As a result, the increase of g_{bs} with LNC was little explained by the alteration of leaf anatomy. In contrast, the combined effect of LNC and leaf age on S_b was responsible for differences in g_{bs} between young leaves and old leaves. Future investigations should consider changes at the level of plasmodesmata and membranes along the CO_2 leakage pathway to unravel LNC and age effects further.

Key words: microstructure, nitrogen content, diffusive resistance, C_4 photosynthesis, image analysis

1. Introduction

Improving the efficiency of photosynthesis could contribute to better food security under an unprecedented rise in global population and climate-change [1,2]. The photosynthesis pathway in C_4 plants enables them to be more efficient in solar-use, nitrogen-use and water-use than C_3 plants [3,4]. In C_4 plants, CO_2 is initially fixed by phospho*enol*pyruvate carboxylase (PEPc) in mesophyll cells, and the resulting metabolites move into the bundle sheath cells where they are decarboxylated into CO_2 and re-fixed by Rubisco. The association of the two cell types, combined with highly regulated enzyme activities, creates a biochemical carbon concentration mechanism (CCM) resulting in an elevated CO_2 concentration nearby the fixation sites of Rubisco [5]. This mechanism effectively suppresses photorespiration, thereby yielding high photosynthetic resource-use efficiencies.

The efficiency of the CCM relies on the concerted action of anatomical, biochemical and biophysical mechanisms [5–8]. It has been well known from C_3 photosynthesis studies that leaf anatomy impact photosynthesis as it influences the physical obstruction to CO_2 diffusion. The leaf boundary layer and stomatal conductances affect diffusion of CO_2 towards the

stomatal cavity. The mesophyll conductance (g_m) constrains the diffusion from sub-stomatal cavities into CO_2-fixation sites in mesophyll. The distribution of stomata and the connectivity of intercellular airspaces affect the diffusion of CO_2 in the gaseous phase, while the properties of the cell wall such as thickness and porosity, the plasma membrane and presence of carbonic anhydrase affect the diffusion in the liquid phase [9–11]. While these phenomena occur in C_4 photosynthesis as well, C_4 photosynthesis is also affected by CO_2 retro-diffusion from bundle sheath cells back into mesophyll cells. This retro-diffusion, also called 'CO_2 leakage', partially increases the CO_2 levels of the mesophyll cells [12] and is constrained by resistance of the mesophyll-bundle sheath interface [13]. The inverse of this resistance is known as the bundle sheath conductance (g_{bs}). The lower g_{bs}, the lower is CO_2 retro-diffusion from bundle sheath cells, and thus the higher is the efficiency of the CCM [5,8,14,15]. Leakiness, a physiological variable often used to characterize retro-diffusion of CO_2 from bundle sheath cells back to mesophyll cells relative to the rate of PEP carboxylation, depends greatly on g_{bs}.

C_4 photosynthetic efficiency has been proposed to depend on a number of anatomical properties of the leaves. For instance, a low permeability of bundle sheath cell walls to CO_2, a high surface of mesophyll cells to volume ratio and features such as close proximity of mesophyll and bundle sheath cells, among others, are essential to the effectiveness of the CCM [5,9,16,17]. Moreover, the shorter vein spacing in C_4 plants than in C_3 plants has been shown to be beneficial for high quantum yields [18]. CO_2 retro-diffusion has also been found to be influenced by the diffusive properties of the stroma and the chloroplast envelope [19]. Thus, the significance of leaf anatomy and ultrastructure of C_4 plants to the efficiency of C_4 photosynthesis continues to be extensively studied [6,16,17,20–23].

CO_2 conductances in C_4 plant leaves were recently estimated using combined gas exchange and chlorophyll fluorescence measurements [24,25] or with carbon isotope discrimination measurements [8,15,25,26] in analogy to the methods used to estimate g_m in C_3 leaves [27–29]. Gas exchange and chlorophyll fluorescence measurements result in CO_2 and irradiance responses of net photosynthesis and quantum efficiency of PSII electron transport, which are then used to parameterize biochemical models of von Caemmerer & Furbank (1999) and estimate g_m and/or g_{bs}. The procedures to estimate these conductances using various software tools are readily accessible [24,32]. In addition, the benefits of chlorophyll fluorescence measurements in C_4 plants have been substantiated [24,25,33,34]. Using these methods, g_{bs} was found to vary with nitrogen supply [24], growth light [7,25,26], leaf age [24,35,36], and temperature [34].

Very few studies measured leaf anatomical properties and estimated g_{bs} or g_m in C_4 plants to examine their relationship [7,26]. These properties include the exposed surface area of mesophyll cells per unit of leaf area (S_{mes}), surface area of bundle sheath cells per unit of leaf area (S_b), leaf thickness and diameter of mesophyll and bundle sheath cells. When maize and *Flaveria bidentis* were grown under contrasting light environment, differences in S_{mes}, S_b (Pengelly *et al*. 2010), leaf thickness and cell diameter (Kromdijk *et al*. 2010) contributed to the variations in g_{bs} or g_m. A negative correlation of bundle sheath resistance with leaf nitrogen content was reported for maize in a recent study [24]. At that time, it was only presumed to be due to S_b and cell wall thickness being altered by nitrogen treatment. In addition, an increase in g_{bs} was suggested when C_4 plants were grown at elevated CO_2 [37] or temperature [38] due to a decrease in wall thickness of the bundle sheath.

The relationships between photosynthesis and leaf anatomical properties have commonly been investigated using chemically fixed leaf tissue samples [6,7,17,39,40]. X-ray micro-computed tomography (X-ray micro-CT) also gives high-quality images that render the airspace between cells at sufficient contrast to allow quantification of anatomical features with the additional advantage of no requirement of intensive sample preparation and thus measurement artefacts are minimized [41–43]. In addition, X-ray micro-CT allows measurements over the intricate three-dimensional leaf geometry of any thickness but has a limitation in resolving leaf ultrastructural components [44,45].

In C_3 plants, it is well known that the cell wall strongly influences CO_2 diffusion and hence CO_2 fixation rate [46]. Whether and how the cell wall of the bundle sheath contributes to the variations in g_{bs} for C_4 plants with leaf nitrogen content and age were not investigated. The objectives of this research were (i) to study how bundle sheath conductance is affected by leaf nitrogen content and leaf age, (ii) to quantify leaf anatomical properties as altered by leaf nitrogen and age using combined microscopy and micro-tomography measurements, (iii) to relate these properties to CO_2 conductances of a maize (*Zea mays* L.) leaf. This will be achieved by using gas exchange and chlorophyll fluorescence measurements with biochemical models of C_4 photosynthesis [30] to estimate g_{bs}, and X-ray micro-CT, light and electron microscopy images to obtain microstructure and ultrastructure details of the leaf anatomy.

2. Materials and methods

2.1. Plants, treatments and photosynthetic measurements

Part of the data of our experiment was used to validate predictions of a C_4 photosynthesis model we presented in a recent publication [12]; therefore, the growth conditions and gas exchange measurements were described therein. In brief, maize (*Zea mays* L.) plants, hybrid 2-02R10074, were grown in a controlled glasshouse in four blocks. In each block, the three nitrogen treatment levels were 0.15 (N1), 0.50 (N2) and 1.25 (N3) g N per pot. There were two leaf ages: 19 d (young leaves) or 32 d (old leaves) counted after their first appearance. For the old leaves, the frequency of applying nutrients was increased to twice weekly after the fourth week (since nutrition application started) to minimize the decline of leaf nitrogen content with leaf age.

Combined gas exchange and chlorophyll fluorescence measurements were done in four replicates on the mid-portion of the 6th leaf, using a LI-6400XT open gas exchange system with an integrated fluorescence chamber head, enclosing a 2 cm^2 leaf area (LI-COR, Lincoln, NE, USA). The CO_2 responses of photosynthesis were measured at an incident light intensity of 1500 µmol m^{-2} s^{-1} in steps of 380, 200, 100, 90, 80, 70, 60, 50, 380, 380, 500, 1000 and 1500 µmol mol^{-1} allowing three minutes per step for photosynthesis to reach a steady-state. The light response curve was measured in leaves that were first dark-adapted for 25 min, in steps of 20, 40, 60, 80, 100, 200, 500, 1000, 1500 and 2000 µmol m^{-2} s^{-1} allowing six minutes per step. The response curves were measured both at 2 % and 21 % O_2, and the IRGA calibration was adjusted for O_2 composition of the gas mixture according to the manufacturer's instructions. The ambient CO_2 was 250 µmol mol^{-1} at 21 % O_2 and 1000 µmol mol^{-1} at 2 % O_2.All measurements were made at leaf temperature of 25 °C and a leaf-to-air vapor difference within 1.0-1.6 kPa, with measurement flow rate of 400 µmol s^{-1}. In addition, using thermally killed leaves, the gas exchange data were corrected for CO_2 diffusion into and out of the leaf cuvette [47]. Simultaneously with the gas exchange measurements, the steady-state fluorescence (F_s) and maximum relative fluorescence (F_m') were also measured. F_s was measured after photosynthesis reached a steady-state after each of the CO_2 or light steps. F_m' was measured after a saturating light-pulse of intensity greater than 8500 µmol m^{-2} s^{-1} for a duration of 0.8 s. The quantum efficiency of PSII electron transport was calculated as $\Delta F / F_m' = (F_m' - F_s) / F_m'$ [48]. Following the photosynthetic measurements, leaf nitrogen content (Micro-Dumas combustion method, Thermo Scientific, elemental C/N analyzer, type:

Flash 2000) and dry mass were determined from three leaf samples (per plant) of having an average area of 2.15 cm^2 that were dried to constant weight in an oven at 70 °C for 48 hr.

2.2. X-ray micro-CT imaging

Maize plants of the same cultivar were grown in three replicates simultaneously with those used in the gas exchange measurement to study the leaf anatomy using microscopy and the tomography experiments. The effect of nitrogen on these plants was assessed from readings of a portable chlorophyll meter (SPAD-502, Minolta, Japan) [49]. Maize leaf tissue samples (5 mm × 5 mm), both for young and old leaves, were obtained from the 6^{th} leaf of each plant. Three samples per plant were taken from six plants (2 ages and 3 N levels). Each leaf was mounted on a polystyrene base and wrapped in a parafilm to prevent dehydration during scanning. The samples were placed on a high precision stage where the sample rotated by 0.4° up to an angle of 196°. The samples were scanned using a high resolution X-ray micro-CT (Skyscan 1172, Bruker micro-CT, Kontich, Belgium) with an operating voltage of 60 kV and a current of 167 µA. Projection images were averaged from three frames. Each frame was captured with a camera size of 2000 x 1048 pixels and $885x10^{-3}$ s exposure time. A single scan lasted for about 30 minutes. The samples were imaged at an isotropic voxel size of 2.96 µm.

Reconstruction of the cross-section from the shadow projections was performed using a filtered back projection algorithm [50] implemented in NRecon 1.6.6.0 (Bruker micro-CT, Kontich, Belgium). Beam hardening correction, smoothing and ring artifact reduction were set at 35, 2 and 8 % respectively. The linear attenuation coefficient range was set at 0 to 0.1068 to improve contrast and to standardize the grayscale range of the output images. The output file was an 8-bit bitmap with about 950 cross-section slices for each data set. The data sets were cleaned to remove noise and other extraneous materials. The cleaning procedure was implemented in the commercial software CTAn v1.13.5.1 (Bruker micro-CT, Kontich, Belgium).

Before morphometric analysis, the images were segmented into the constituent objects by using Otsu's algorithm [51] in CTAn. A common global threshold value of 63 was found suitable for segmentation of the intercellular airspaces from cells of the leaf types. The segmented images were subsequently analyzed using a 3-D algorithm to determine the tissue volume, porosity, pore (intercellular airspace) surface per volume, connectivity density of the pores and leaf thickness [41].

2.3. Light and electron microscopy measurements

Leaf samples from the 6th leaf, both young and old, were fixed in cold 2 % glutaraldehyde, buffered at pH 7.3 with 50 mM Na-cacodylate and 150 mM saccharose. Post fixation was carried out in 2 % osmium tetroxide in the same buffer. After dehydration in a graded acetone series, tissues were embedded in Araldite and sectioned with a Leica EM UC6 ultra-microtome. Serial semi-thin sections with a thickness of 1 µm were stained with methylene blue and thionin and viewed in an Olympus BX-51 microscope at 40x. Double stained 70 nm thin sections were examined in a Zeiss EM900 electron microscope.

Anatomical parameters such as S_{mes}, S_b and the interveinal distance were measured from the light microscopy images while the cell wall thicknesses of mesophyll and bundle sheath were obtained from electron microscopy images. Three image samples were randomly selected for each N treatment × leaf age combination. The images were first digitized using in-house-made software [52]. The digitized images were then imported into finite-element software Comsol Multiphysics vs. 3.5 (Comsol AB, Stockholm). To calculate S_{mes} and S_b the length of exposed mesophyll surface, perimeter of bundle sheath cells within an interveinal distance and a leaf area, taken as a distance between the centers of two consecutive bundle sheath cells, were measured [7]. Using a curvature correction factor of 1.43 [53,54], these dimension measurements were converted into area. The thicknesses of mesophyll and bundle sheath cells wall were taken as the average of the distance between several parallel points on the digitized images of the cell walls. Interveinal distance was measured as the distance between the centers of two successive veins per image sample.

2.4. Estimation of bundle sheath conductance and other parameters

We used the procedure of Yin *et al*. [24] to estimate g_{bs} and other photosynthesis parameters. The underlying model equations of the procedure are listed in supplementary Text S1 while model input parameters are shown in Table S1. Using the method developed previously [24], the rate of day respiration (R_d) was estimated as the intercept of the linear relationship between photosynthesis and the term $I_{inc}\Phi_2/3$, based on data from the light-

response curves at low ranges of an incident light intensity (I_{inc}) ($20 \leq I_{inc} \leq 200$ µmol m^{-2} s^{-1}). The measurements at 2 and 21 % O_2 levels were pooled to estimate a common R_d since the estimate for each O_2 level did not differ significantly ($P > 0.05$). The slope of the same linear regression but using data of 2 % O_2 plus measurements from the CO_2 response curves at high CO_2 ranges (≥ 500 µmol mol^{-1}) at 2 % O_2 could give the lumped calibration factor $s´$ for calculating potential ATP production rate J_{ATP} (Eq. S2, Supplementary materials), based on fluorescence measurements [24]. Here, $s´$ was estimated for each leaf type simultaneously with g_{bs} as described below.

Bundle sheath conductance values corresponding to the three N levels × two leaf ages were determined using the SAS (SAS Institute Inc., Cary, NC, USA) code obtained from Yin *et al*. [24] (the code is available upon request to the corresponding author of that paper). To avoid overfitting, we assumed a linear relationship between g_m and leaf nitrogen content (LNC) as was also shown to exist for C_4 crops [24,55]. The common slope of linearity (X_{gm}) was estimated (for details, see Text S1, Supplementary materials). In addition, we found a good linear relationship between the quantum efficiency of CO_2 fixation and that of PSII electron transport (Fig. S2, Supplementary materials) across all light and CO_2 levels. This suggests that (i) the proportion of ATP or energy used for sinks other than CO_2 fixation was not altered during the measurements, and, more importantly, (ii) any enzymatic limitation, if occurred, had a feedback effect on electron transport. Consequently, most of the measured rates of photosynthesis were covered by equations of electron-transport-limited rates of the model (Eq. S1 and Eq. S5). Therefore, the resulting estimates for maximum catalytic rate of PEPc ($V_{p,max}$) and ribulose-1,5-bisphosphate carboxylase/oxygenase (Rubisco) ($V_{c,max}$) were not well constrained and had unreasonably high standard errors. This had little impact as the main aim here was not to estimate $V_{p,max}$ or $V_{c,max}$ but g_{bs}. Thus, we fixed $V_{p,max}$ and $V_{c,max}$ to arbitrarily high values to estimate g_{bs}, $s´$ and X_{gm} only. Furthermore, it was shown recently that the use of a rectangular flash in a chlorophyll fluorescence measurement resulted in an underestimation of quantum efficiency of PSII electron transport, Φ_2 [56]. However, the influence of this underestimation is minimized using our calibration procedure for calculating J_{ATP}. For example, a 20 % higher Φ_2 [56] would lower the estimated $s´$ by ca. 16 %. As a result, J_{ATP} is minimally affected (see Eq. S2, Supplementary materials) as $s´$ compensated, to some extent, for an underestimation in Φ_2 [33]. Thus, the estimated g_{bs} values did not change (Table S2, Supplementary materials).

2.5. Statistical analysis

A number of leaf anatomical properties for the six leaf age × N combinations were measured to determine explanatory variables for variation in g_{bs}. Using principal component analysis, the data of mean values could be summarized into linear combination of a few key variables that contribute to the variability in data while elucidating the relationship between leaf anatomical parameters and the g_{bs} and g_m. ANOVA was carried out using JMP version 12 (SAS Institute, USA) to compare N and leaf age groups. Mean values of the leaf morphometric parameters were then compared using student's t-test. A significance level of 5 % was used for this analysis.

3. Results

3.1. Effect of nitrogen supply and leaf age on photosynthesis

The effect of increased N supply and leaf aging on the rate of photosynthesis (A) in response to intercellular CO_2 concentration (C_i) and I_{inc} are shown in Fig. 1 and Fig. 2, respectively. Fig. 1 and Fig. 2 show that A increased with the amount of N added to the pots and declined with leaf age. These effects were reflected in the measured responses Φ_2 (Fig. 3) which were high for N3 leaves at high I_{inc} values and lower in old leaves than young leaves. The oxygen level, 2 % or 21 %, did not affect A and Φ_2 substantially although the differences in A and tends to be more in young N3 leaves suggesting an increased photorespiration. Therefore, higher N application increased A and Φ_2 while leaf aging decreased them, as expected.

3.2. The relationship between photosynthetic characteristics and LNC

Table 1 shows that the LNC increased in proportion to the amount of N added to the pots. Leaf aging decreased the LNC, however, less so for N2 and N3 leaves as a result of the more frequent N treatments for the old leaves. All young leaves had significantly higher A than all old leaves while all N3 leaves had significantly higher A than N2 and N1 leaves (Table 1). The relationships between A, day respiration rate (R_d), leaf dry mass per leaf area (LMA), light conversion efficiency (s') and LNC are shown in Fig. 4. There was a strong positive correlation between A and LNC. LMA declined as LNC increased. R_d generally increased with LNC but the correlation was weak. There was also a loose correlation between s' and LNC. The correlation of A with LNC was significant.

3.3. Bundle sheath conductance in response to LNC and leaf age

Table 1 shows that estimated g_{bs} values were higher for N3 leaves than for N2 and N1 leaves. Old leaves had lower g_{bs} than young leaves. The model to estimate g_{bs} predicts the rate of photosynthesis well (Fig. 1 and Fig. 2, $r^2 = 0.98$); however, some of the best-fit values of g_{bs} had higher standard errors. Although there is uncertainty on the actual g_{bs}, the estimated values show a general trend of increasing with LNC and declining with leaf age. In addition, g_{bs} correlated with LNC ($r^2 = 0.90$) (Fig. 5). Across N levels and leaf ages, the bundle sheath resistance thus varied from ca. 281 to 2756 m^2 s mol^{-1}. Furthermore, the estimated X_{gm} was 2.83 ± 0.16 mol $(g\ N)^{-1}$ s^{-1} resulting in g_m values of 0.54 mol m^{-2} s^{-1} at the lowest LNC and 2.85 mol m^{-2} s^{-1} at our highest LNC.

As a result of increased g_{bs} with LNC, the mean CO_2 concentration in the bundle sheath (C_c) (Fig. 6) was higher for young N1 leaves than for young N2 and N3 leaves across all irradiances. This pattern was the same for the old leaves (Fig. S4, Supplementary materials). Across leaf ages, C_c was higher in old leaves than in young leaves consistent with differences in g_{bs} (Fig. S4, S5, Supplementary materials). The efficiency of the CCM as indicated by leakiness, however, was not substantially different within N levels (Fig. 6). The predicted leakiness was also similar across leaf ages (Fig. S6, S7, Supplementary materials).

3.4. Sensitivity analysis

The sensitivity of X_{gm}, $s´$ and g_{bs} to the fraction of ATP allocated to the C_4 cycle (x) (Table S1), which is an important determinant of the electron-transport-limited rate of PEP carboxylation and photosynthesis (Eq. S1 and Eq. S5, Supplementary materials), is shown in Table S4 (Supplementary materials). The estimated X_{gm} and s' were largely insensitive to various values of x except when it was low (0.35). However, the value $x = 0.35$ may not be biologically realistic as many modeling studies show that x is very close to 0.40 [24,57] under various treatments and ambient conditions. Yin & Struik [58] estimated that when additional ATP utilizing processes were considered, x varies from 0.399 to 0.385. Optimization analysis showed that the optimum x was ca. 0.4 over a wide range of conditions, except under extremely low-light conditions [57]. Table S4 also shows that g_{bs} was sensitive to x. However, when x was also estimated simultaneously with g_{bs} from our model (not shown), it was 0.43 ± 0.042 which is also close to 0.4. We decided to fix $x = 0.4$ to improve the estimation of g_{bs} by reducing the number of parameters to be fitted. Fig. S3 (Supplementary materials) shows that the relationship between g_{bs} and LNC remained strongly linear. Therefore, although the

estimated g_{bs} values were sensitive to the choice of x, the relationship between g_{bs} and LNC was minimally affected. The magnitudes of leakiness and C_c were, however, sensitive to x (Fig. S8 and Fig. S9, Supplementary materials). Therefore, these predictions should be considered as temporary values. However, the trends of C_c and leakiness were not altered. Furthermore, X_{gm}, s' and g_{bs} were expectedly insensitive to Rubisco and PEPc kinetics parameters (Table S1, Supplementary materials) due to the close link between photosynthesis and electron transport (Fig. S10, Supplementary materials).

3.5. The effects of LNC and leaf age on the anatomy of maize leaves

Table 2 shows the measurement results of the leaf morphological properties for young and old leaves. The portable chlorophyll meter readings that correlate with chlorophyll content [49], were higher for N3 and N2 than for N1 leaves and lower for old leaves than for the young leaves (Table 2). This implies that the nitrogen content of maize leaves used for imaging increased with higher N application and decreased with leaf age. The images of transverse sections of the maize leaf samples, cell walls of the bundle sheath and surface rendering of leaves using x-ray micro-CT images are shown in Fig. S11, Fig. S12 and Fig. S13, respectively (Supplementary materials).

Anatomical parameters such as S_{mes}, S_b, leaf thickness, cell volume and bundle sheath cell wall thickness were not significantly altered by LNC. Old N1 leaves had a significantly thicker mesophyll cell wall than old N2 leaves. The pore surface to volume ratio of young N1 leaves was significantly higher than that of young N2 and N3 leaves while it was significantly larger for old N1 leaves than for the old N2 leaves. Old N3 leaves were significantly more porous than old N2 leaves. The connectivity density was significantly larger in the old N3 leaves than that in the N2 leaves. Both young and old N1 leaves had significantly shorter interveinal distance that N2 and N3 leaves.

The porosity, pore surface per volume and connectivity density values were not significantly different between young and old leaves. Young N1 leaves were significantly thicker than old N1 leaves. Old N1 leaves had significantly thicker cell walls of mesophyll and bundle sheath than young N1 leaves. Comparing across leaf ages, mean values of S_{mes} of old leaves were larger than those of young leaves. However, statistical analysis showed that only old N2 leaves had a significantly larger S_{mes} than young N2 leaves. In contrast, all young leaves had significantly higher S_b than their respective old leaves. The difference in inteveinal distance between young and old N1 leaves was significant.

3.6. Bundle sheath conductance in relation to leaf anatomy

The correlation between the measured leaf anatomical parameters and g_{bs} is shown by principal component analysis (PCA) biplot in Fig. 7 in analogy to a study on C_3 plants [59]. The scores represent young and old leaves. Since a total of six g_{bs} values were estimated for LNC × leaf age combinations, mean values of anatomical parameters were used in PCA. The direction of correlation loadings which are vectors with origin at (0,0) shows positive or negative correlation. Thus, the vectors in opposite direction are largely negatively correlated while the vectors pointing to the same direction are positively correlated. If the vectors point in the direction of a score (young or old leaves), the score is characterized by a positive value of the corresponding anatomical property or CO_2 conductance. Vectors that are perpendicular to each other are uncorrelated. The corresponding correlation coefficients are shown in Table S3 (Supplementary materials).

The PCA analysis resulted in 2 principal components (PCs) that explained 82 % of the total variance. PC1 was well correlated ($r > 0.70$) to cell wall thickness of mesophyll and bundle sheath cells, S_{mes}, S_b, leaf thickness and tissue volume (Table S3, Supplementary materials). Thus, PC1 was correlated to the major determinants of g_{bs} and g_m. The first PC was also effective in separating young and old leaves. g_m, g_{bs} and porosity are highly correlated similar to the correlation between leaf thickness, S_b and cell volume. g_{bs} is correlated with interveinal distance and S_b although less strongly than leaf thickness. There was a strong negative correlation between the mesophyll cell wall thickness and g_m but not g_{bs}. The bundle sheath cell wall thickness was inversely related to g_{bs} while S_{mes} was inversely related to g_m. Void surface per volume and connectivity density were correlated to each other but uncorrelated to other anatomical properties and g_m in this biplot. Fig. 7 also shows that old leaves in general have thicker cell walls of mesophyll and bundle sheath cells, lower conductances and are thinner than young leaves.

4. Discussion

4.1. Bundle sheath conductance increased with LNC and declined with leaf age

We have grown maize plants under three nitrogen treatment levels to study how g_{bs} varies with LNC. Previously, it was shown that g_{bs} increased with LNC for two extreme N treatment levels [24]. Our results confirm that g_{bs} varied in proportion to LNC (Table 1). The bundle sheath resistances were mostly in the range 100 to 1600 m^2 s mol^{-1}, reported for various C_4

species [19,24,26,60]. More importantly, g_{bs} significantly correlated with LNC while the impact of the latter on g_{bs} was much more than that of leaf age as confirmed by a two-variable regression. The effect of decreased CO_2 concentration in bundle sheath cells due to high g_{bs} with high LNC was reflected in the fraction of assimilation lost due to photorespiration (Eq. S13, Supplementary materials) which was higher for N3 leaves than N1 and N2 leaves (Fig. S14, Supplementary materials). In addition, leakiness was not affected by the LNC since the energy efficiency of CO_2 fixation indicated by the ratio of quantum yield of CO_2 fixation to quantum yield of PSII electron transport was not significantly different in young and old leaves within N levels (Fig. S15, Supplementary materials). Consistent with this, the predicted leakiness (Fig. 6) also shows that the efficiency of the C_4 cycle was not substantially affected while a strong positive correlation between A and LNC was found (Fig. 4). This occurs when the increased rate of CO_2 leakage was matched with increased delivery of CO_2 by the higher capacity of the C_4 cycle in leaves having high LNC. Consequently, the bundle sheath resistance of high photosynthesis capacity leaves should decrease [19]. The corollary to these predictions is that the maize plants grown in low N supply responded by increasing bundle sheath resistance to maintain similar efficiency. This raises the question of how the variation of g_{bs} was achieved.

4.2. The combined effect of LNC and leaf age on anatomy may explain the differences in bundle sheath conductance

Our results for the increase of g_{bs} with LNC (Fig. 5) confirm the earlier result of Yin *et al*. [24] based on only two nitrogen treatments. This positive correlation could be examined using the influence of LNC on anatomical components of g_{bs}, S_b, and cellular conductance, which is the CO_2 conductance of the mesophyll-bundle sheath interface [30]. The cellular conductance may be expected to be influenced by properties of the bundle sheath cell wall, while g_{bs}, which is expressed per unit leaf area, is influenced by S_b [30]. The measured S_b was in the range of values reported in the literature 1.5 to 3.1 m^2 m^{-2} [6,7,17,61,62]. In addition, the measured values of cell wall thickness of bundle sheath cells are close to the reported values for C_4 plants, including maize, ca. 0.3 to 1.6 μm [19,37,63,64]. The decline of g_{bs} with leaf aging was accompanied by a significant decline of S_b. Due to this reduction in S_b, old leaves were also significantly thinner than young leaves except for old N2 leaves, where the reduction in S_b accompanied by significantly larger S_{mes} resulted in similar leaf thickness (Table 2). In old N1 leaves, particularly, the wall thickness of bundle sheath cells was also thicker. Since LNC also declined with leaf age (Table 1), significantly so within young and

old N1 leaves, these responses of leaf anatomy and the resulting differences in g_{bs} are attributed to the combined effects of LNC and leaf age. However, within N levels, it seems that neither S_b nor wall thickness of bundle sheath was responsible for the differences in g_{bs}. The anatomy changed in such a way that only the vein spacing increased with LNC but interveinal distance correlated to g_{bs} less strongly. The lack of association between g_{bs} and cell wall thickness within N levels suggests that other factors may play a role. For instance, the density of plasmodesmata which are considered the main pathway to CO_2 leakage [64,65] since the suberin layer (for instance, Fig. S16, Supplementary) may restrict the leakage of CO_2 through the cell walls as suggested previously [66,67]. Previous reports show that the abundance of plasmodesmata responded to growth conditions such as low temperature or low irradiance [20,68]. Overall, the impact of LNC on g_{bs} was not due to alteration of the anatomical factors while its effect on the anatomy in interaction with leaf age explains for differences in g_{bs} between young and old leaves.

4.3. Mesophyll conductance in relation to LNC and leaf age

In C_3 plants, a positive correlation of g_m with exposed mesophyll surface has been reported [46]. For C_4 plants, CO_2 assimilation occurs in the mesophyll cytosol, thus the parameter S_{mes} is believed to be positively related to g_m [19]. Our measured S_{mes} was in the range of values reported for C_4 species [6,16,62]. In relation to g_m, however, S_{mes} did not change significantly with LNC. S_{mes} had also strong negative correlation with g_m (Fig. 7) due to a higher S_{mes} in old leaves than young leaves. Thus, the role of S_{mes} in g_m was counter-intuitive. As shown in Fig. 7, g_m also correlated with porosity, leaf thickness and mesophyll cell wall thickness. The lack of significant differences in porosity or degree of connectivity of airspaces in many of the leaves, however, rules out the possibility of causal relationship between the parameters and variations in g_m. In addition, since maize is an amphistomatous leaf, the resistance of the intercellular airspace resistance is low [69]. Among young and old leaves, the decline of leaf thickness may have been due to reduced S_b not due to changes in S_{mes}. A strong negative correlation of mesophyll cell wall thickness with g_m in combination with a significantly thicker mesophyll cell wall of old N1 leaves support the decline of g_m across leaf ages.

4.4. Implications of conserved leaf anatomy under contrasting LNC on photosynthesis

An increased g_{bs} with LNC reduced the effectiveness of the CCM as the CO_2 concentration in the neighborhood of Rubisco decreased. On the other hand, similar to

previous reports [70–72], higher LNC boosted the rate of photosynthesis. In addition, high LNC leaves had low LMA which is associated with elevated concentration proteins and photosynthesis [73]. It is to be noted that our measured photosynthesis was mainly limited by electron transport. This paradox could be explained by the increase in quantum efficiency of electron transport outweighing the increase of g_{bs} with LNC. In conjunction with leaf anatomical data, this implies that the negative impact of decreased bundle sheath resistance was not detrimental to the rate of photosynthesis. Similarly, Yin *et al*. [24] have shown that the increase of g_{bs} by LNC has less influence on the rate of photosynthesis compared to the effect of LNC on photosynthetic capacity. It could also be that increased CO_2 leak with high LNC may elevate the CO_2 concentration in mesophyll [12], thus, the rate of PEP carboxylation and maintains balance of energy supply and demand, boosting photosynthesis [74].

In response to growth conditions, some C_4 plants have shown to respond, for instance, through alteration in anatomy [7,26]. Similarly, due to leaf aging, which was accompanied by a drop in LNC, old maize leaves had lower g_{bs} than young leaves through lower S_b. However, the anatomy of maize leaf was generally conserved despite the large differences in LNC (Table 2). While accepting that the tissue preparation for the microscopy experiment may have affected our results, the apparent lack of effect of LNC may also be in line with the hypothesis that coordinated changes in leaf anatomy in response to environmental changes ensuring intimate contacts of mesophyll and bundle sheath cells are essential efficient metabolite transport, thus, CCM [16,39,66,75]. These views suggest that the leaf anatomy in C_4 plants may be constrained by the need for rapid metabolite fluxes.

We investigated the bundle sheath conductance in relation to anatomy of maize leaf as a function of nitrogen and leaf age. g_{bs} was strongly related to LNC but leaf anatomy was not. Consequently, changes in the leaf anatomy were not the cause of variation in g_{bs} with LNC except in interaction with leaf age. This was unexpected and counter-intuitive. However, since the chloroplast envelope and plasma membrane also contribute to bundle sheath resistance, the possible effect of nitrogen through altered composition, thus permeability, should be accounted for. The CO_2 diffusion in the liquid phase of mesophyll cells is also constrained by the permeability of the plasma membrane which, in maize, contains aquaporins and carbonic anhydrases that may enhance its CO_2 permeability [76,77]. Therefore, future investigations considering these components along with the roles of suberin and plasmodesmata are recommended to unravel the effect of LNC on g_{bs} further.

5. Acknowledgments

The authors thank the Research Council of the K.U. Leuven (OT 12/055) and the Research Fund Flanders (project G.0645.13) for financial support.

Figure captions

Figure 1. The response of photosynthesis to intercellular CO_2 concentration (C_i) for young (A1) and old (A2) leaves from maize plants grown under three nitrogen (N) levels: low (N1); intermediate (N2) and high (N3). Symbols show measured values while curves show model predicted values connected. Each measurement value is an average of measurements in four replicates (Materials and methods). The bars show standard error of the measurements. The oxygen levels were 21 % (filled circles, solid curves) and 2 % (open circles, dashed curves). The irradiance was kept at 1500 µmol m^{-2} s^{-1}.

Figure 2. The response of photosynthesis to incident irradiance for young (A1) and old (A2) leaves from maize plants grown under three nitrogen (N) levels: low (N1), intermediate (N2) and high (N3). Symbols show measured values while curves show model predicted values connected. Each measurement value is an average of measurements in four replicates (Materials and methods). The bars show standard error of the measurements. The oxygen levels were 21 % (filled circles, solid curves) and 2 % (open circles, dashed curves). The ambient CO_2 was kept at 250 µmol mol^{-1} for 21 % and 1000 µmol mol^{-1} for 2 % oxygen levels.

Figure 3. The measured response of apparent quantum efficiency of PSII electron transport to intercellular CO_2 concentration (top) and incident irradiance (bottom) for young (filled symbols) and old (open symbols) leaves at three nitrogen (N) levels: low (N1), intermediate (N2) and high (N3). The oxygen levels were 21 % (circles) and 2 % (triangles). The irradiance was kept at 1500 µmol m^{-2} s^{-1}. The bars show standard error of the measurements (n = 4).

Figure 4. Photosynthesis rate (A), day respiration (R_d), leaf dry mass per leaf area (LMA) and light conversion efficiency ($s´$) in relation to leaf nitrogen content (LNC). Open circles represent the young leaves while open circles show old leaves.

Figure 5. The estimated bundle sheath conductance (g_{bs}) values of young (filled circles) and old leaves (open circles) in relation to leaf nitrogen content (LNC).

Figure 6. The predicted response of mean concentration of CO_2 in bundle sheath cells (C_c) (left panel) and leakiness (right panel) to incident irradiance (I_{inc}) for young leaves grown at

three nitrogen (N) levels: low (N1, square), intermediate (N2, circle) and high (N3, triangle). The ambient CO_2 was kept at 250 µmol mol^{-1} and oxygen level was 21 %.

Figure 7. Principal component analysis (PCA) biplot of young and old leaves showing the grouping of leaf types in terms of leaf anatomical properties (mean values). Scores of young (A1) and old leaves (A2) grown under three nitrogen (N) levels: low (N1), intermediate (N2) and high (N3) are shown. Variables should be interpreted as vectors with origin in (0,0). Correlation loading (+) located between the circles (70 % and 100 % of the explained variance limits) are considered most important for explaining the variability with respect to the principal component shown. Correlation between variables is as follows; variables with correlation loadings that are close to each other are correlated, loading that are 90° from each other are uncorrelated and loading that are 180° from each other are inversely correlated. Abbreviations: bundle sheath (BS) conductance (g_{bs}), mesophyll (M) conductance (g_m), exposed mesophyll surface per unit leaf area (S_{mes}), bundle sheath surface area per unit leaf area (S_b).

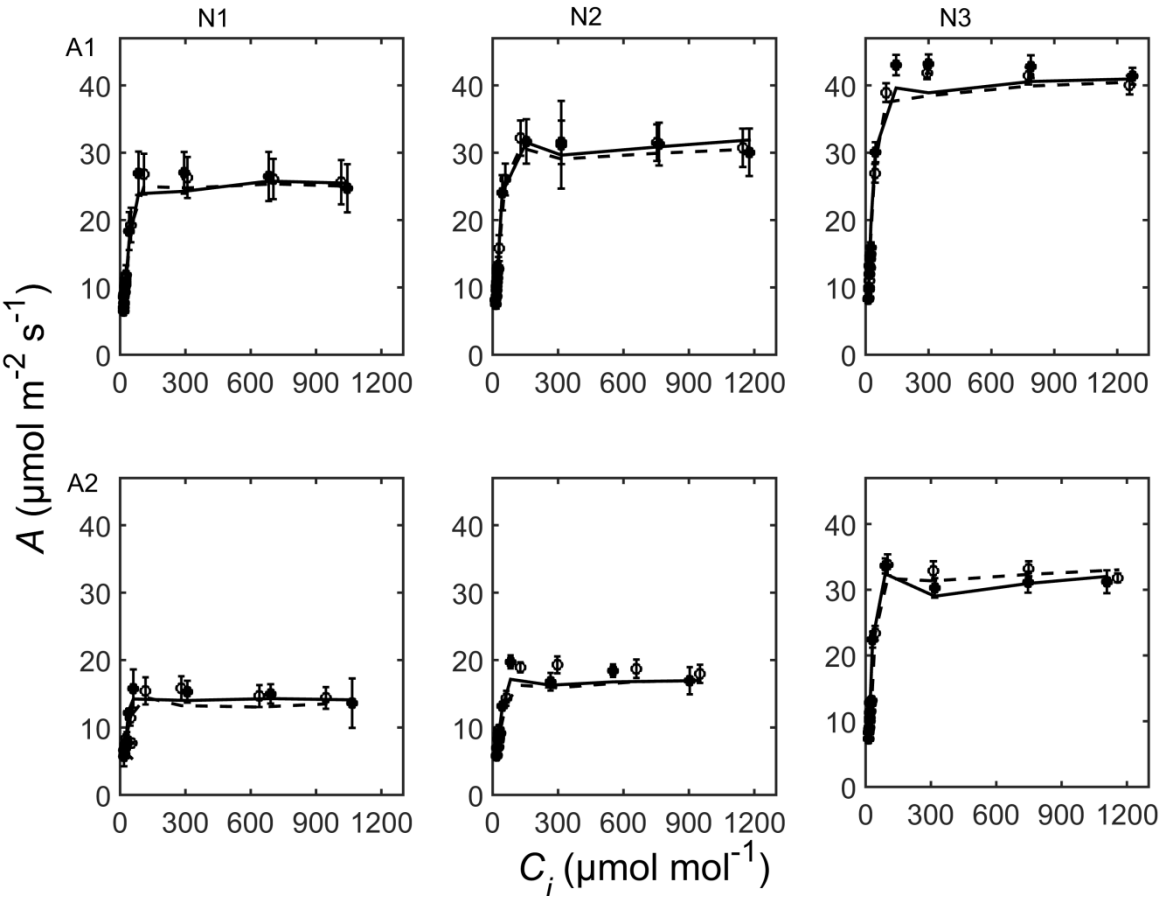
N1
N2
N3
A1
A2
A (μmol m-2 s-1)
Ci (μmol mol-1)
0
10
20
30
40
0
300
600
900
1200

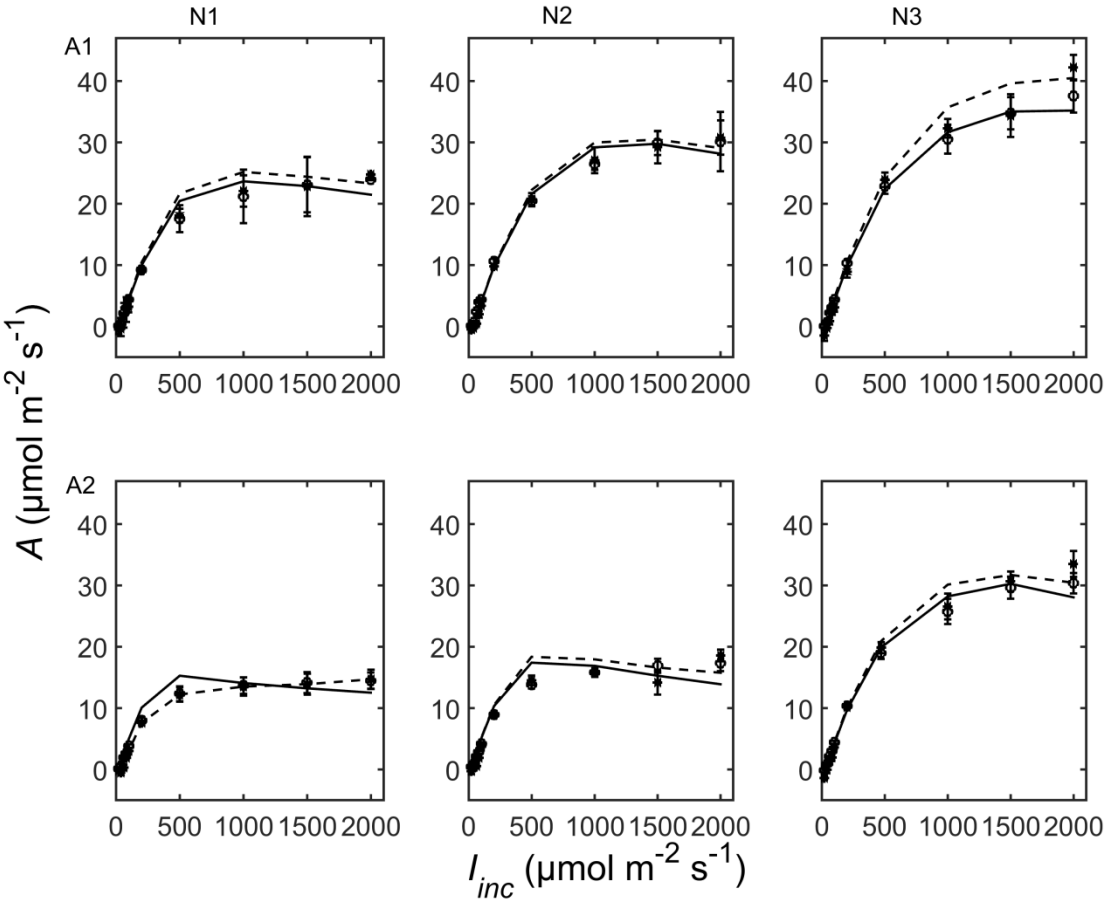
N1
N2
N3
A1
A2
A (μmol m-2 s-1)
Iinc (μmol m-2 s-1)
0
10
20
30
40
0
500
1000
1500
2000

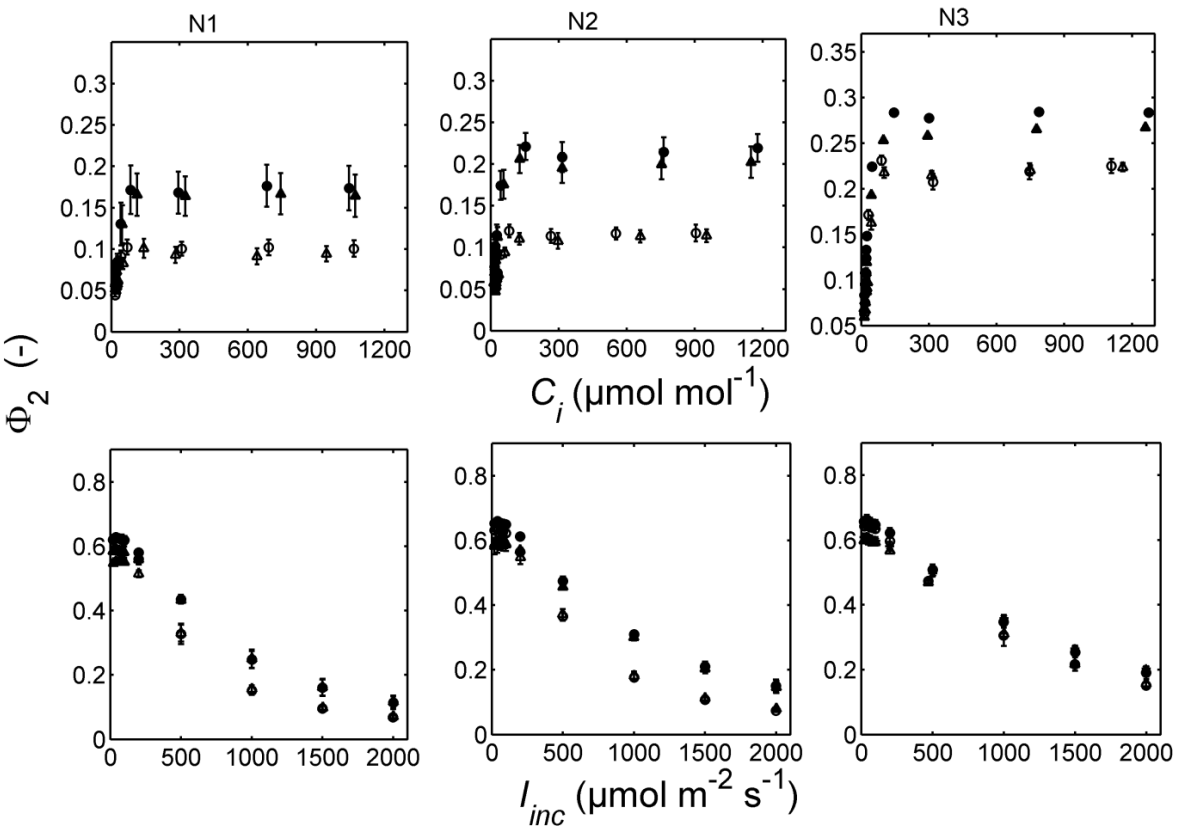
N1
N2
N3
Φ2 (-)
Ci (µmol mol-1)
Iinc (µmol m-2 s-1)

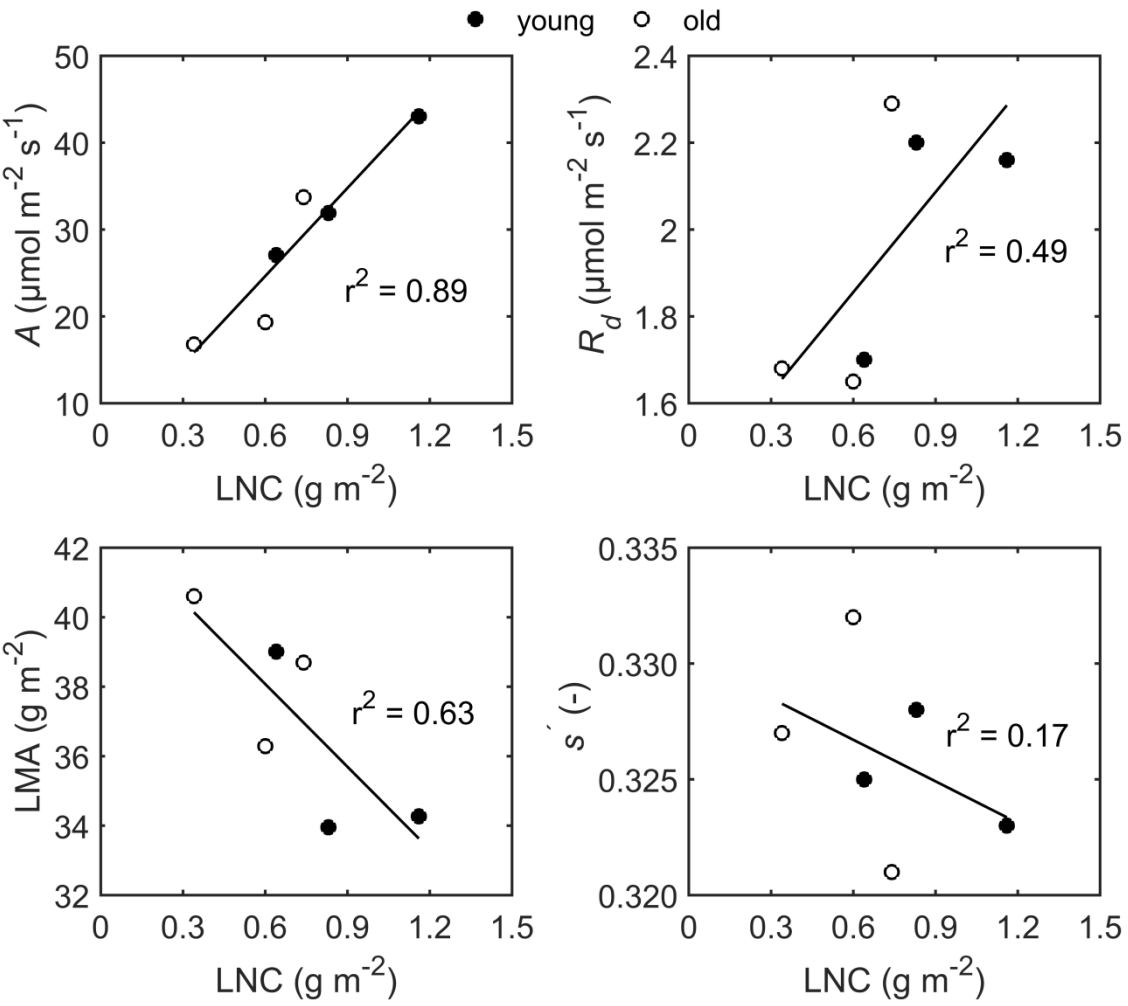
young
old
A (μmol m-2 s-1)
r2 = 0.89
LNC (g m-2)
Rd (μmol m-2 s-1)
r2 = 0.49
LNC (g m-2)
LMA (g m-2)
r2 = 0.63
LNC (g m-2)
s´ (-)
r2 = 0.17
LNC (g m-2)

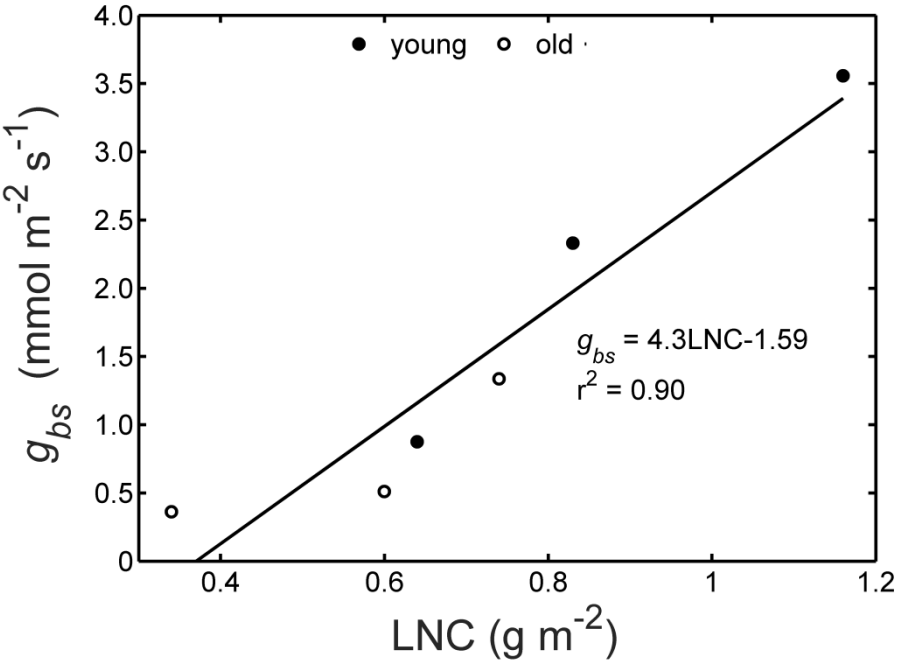
young
old
g_{bs} = 4.3LNC-1.59
r^2 = 0.90
g_{bs} (mmol m^{-2} s^{-1})
LNC (g m^{-2})
4.0
3.5
3.0
2.5
2.0
1.5
1.0
0.5
0
0.4
0.6
0.8
1
1.2

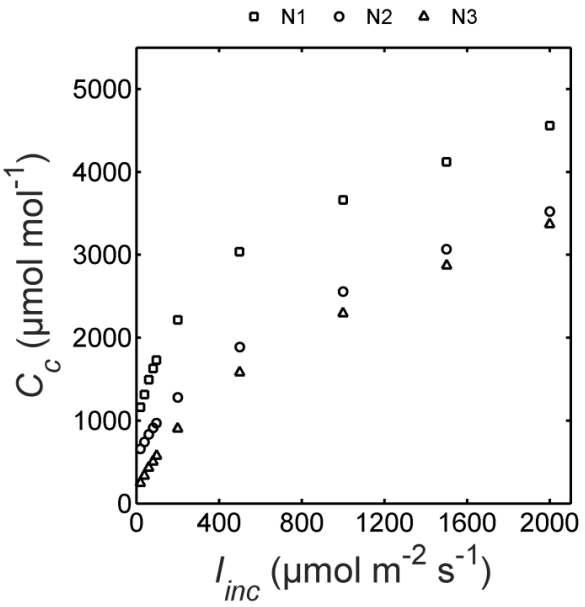
N1
N2
N3
C_c (µmol mol^{-1})
I_{inc} (µmol m^{-2} s^{-1})
0
1000
2000
3000
4000
5000
0
400
800
1200
1600
2000

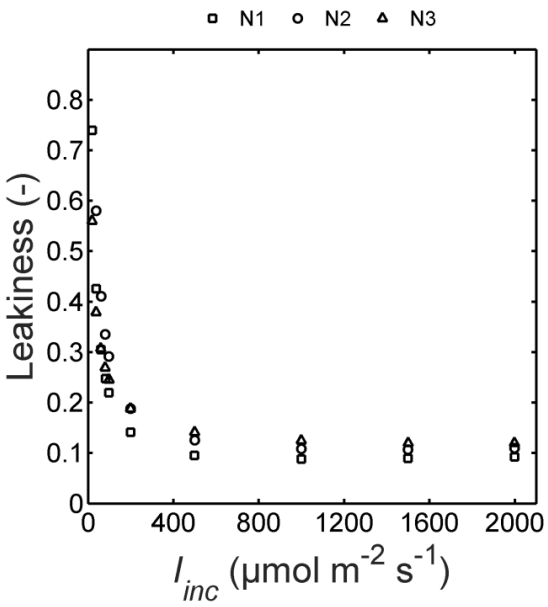
N1
N2
N3
Leakiness (-)
I_{inc} (µmol m^{-2} s^{-1})
0
0.1
0.2
0.3
0.4
0.5
0.6
0.7
0.8
0
400
800
1200
1600
2000

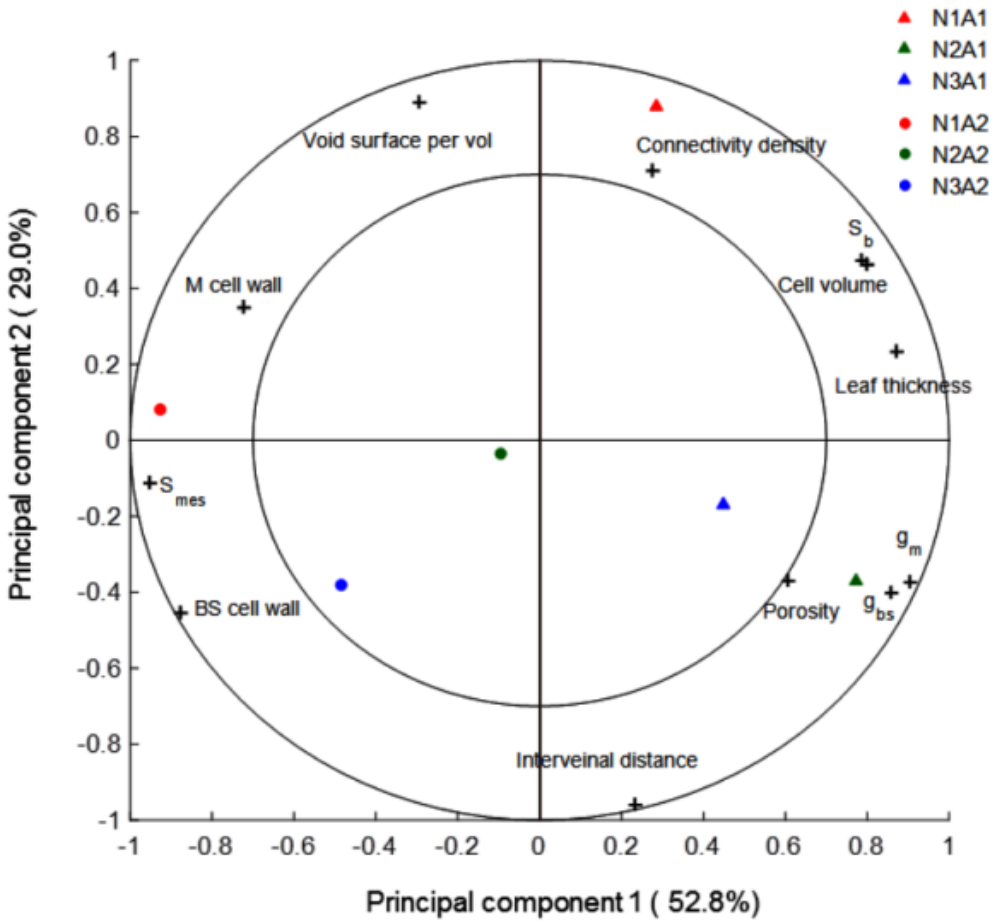
N1A1
N2A1
N3A1
N1A2
N2A2
N3A2
Void surface per vol
Connectivity density
S b
Cell volume
M cell wall
Leaf thickness
S mes
g m
BS cell wall
Porosity
g bs
Interveinal distance
Principal component 2 (29.0%)
Principal component 1 (52.8%)
1
0.8
0.6
0.4
0.2
0
-0.2
-0.4
-0.6
-0.8
-1
-1
-0.8
-0.6
-0.4
-0.2
0
0.2
0.4
0.6
0.8
1

Table captions

Table 1. Estimated values of R_d, s' and g_{bs} (mean ± standard error, n=4) for young (A1) and old (A2) leaves from maize plants grown under three nitrogen (N) levels: low (N1), intermediate (N2) and high (N3). Shown also are leaf nitrogen content (LNC), leaf mass per unit leaf area (LMA) and net photosynthesis (A) at ambient CO_2 of 380 µmol mol^{-1}, 21 % O_2 and irradiance of 1500 µmol m^{-2} s^{-1}. Means not connected by the same letter are significantly different ($P < 0.05$). Comparisons between leaf ages are indicated by upper case letters while differences among N levels within an age level are indicated by lower case letters.

Leaf age	Leaf type	LNC g m^{-2}	LMA g m^{-2}	A µmol m^{-2} s^{-1}	R_d µmol m^{-2} s^{-1}	s'	g_{bs} mmol m^{-2} s^{-1}
A1	N1	0.64±0.09 a,A	39.01±0.65 a,A	27.05±2.79 a,A	1.70±0.20	0.325±0.004	0.88±0.55
	N2	0.83±0.08 a,A	33.95±0.59 b,A	31.92±2.34 a,A	2.20±0.23	0.328±0.003	2.33±0.83
	N3	1.16±0.12 b,A	34.27±0.93 b,A	43.04±1.31 b,A	2.16±0.27	0.323±0.006	3.56±0.90
A2	N1	0.34±0.03 a,B	40.60±1.55 a,A	16.78±1.40 a,B	1.68±0.17	0.327±0.007	0.36±0.50
	N2	0.60±0.11 a,A	36.29±1.72 a,A	19.33±0.80 a,B	1.65±0.21	0.332±0.003	0.51±0.51
	N3	0.74±0.15 a,A	38.70±2.30 a,A	33.74±0.99 b,B	2.29±0.19	0.321±0.003	1.34±0.62

Table 2. Leaf anatomical properties of young leaves (A1) and old leaves (A2) (mean ± standard error, n=3) from maize plants grown under three nitrogen (N) levels: low (N1), intermediate (N2) and high (N3). Means not connected by the same letter are significantly different ($P < 0.05$). Comparisons between leaf ages are indicated by upper case letters while differences among N levels within an age level are indicated by lower case letters. Porosity, cell volume, pore surface per volume, connectivity density and leaf thickness were measured from X-ray micro-CT images. Cell wall thicknesses were measured from transmission electron microscopy images. S_{mes}, S_b and interveinal distances were measured from light microscopy images.

Parameter	A1			A2		
	N1	N2	N3	N1	N2	N3
Chlorophyll meter readings (SPAD units)	38.1	42.3	48.1	22.1	27.2	39.4
Porosity (%)	36.7 ± 0.39 a,A	38.3 ± 1.1 a,A	38.6 ± 2.5 a,A	37.05 ± 2.6 ab,A	36.3 ± 0.25 a,A	38.4 ± 0.53 b,A
Cell volume	1.79 ± 0.04 a,A	1.66 ± 0.05 a,A	1.68 ± 0.05 a,A	1.46 ± 0.04 a,B	1.58 ± 0.05 a,A	1.61 ± 0.1 a,A
Pore surface/volume (mm^2 mm^{-3})	268 ± 0.60 a,A	255 ± 0.59 b,A	253 ± 5.1 b,A	261 ± 3.7 a,A	258 ± 1.2 b,A	263 ± 7.7 ab,A
Connectivity density ×1000 (mm^{-3})(1)	81.9 ± 1.2 a,A	78.9 ± 4.7 a,A	77.8 ± 8.1 a,A	78.5 ± 9.1 ab,A	74.0 ± 1.5 a,A	81.6 ± 2.2 b,B
Leaf thickness (µm)	237 ± 6.87 a,A	217 ± 8.41 a,A	243 ± 7.84 a,A	197 ± 5.22 a,B	209 ± 8.91 a,A	208 ± 5.31 a,A
Bundle sheath cell wall thickness (µm)	0.188 ± 0.0140 a,A	0.245 ± 0.0458 a,A	0.260 ± 0.0331 a,A	0.457 ± 0.0190 a,B	0.445 ± 0.0500 a,A	0.319 ± 0.0150 a,A
Mesophyll cell wall thickness (µm)	0.161 ± 0.0277 a,A	0.119 ± 0.0209 a,A	0.138 ± 0.0288 a,A	0.230 ± 0.0277 a,B	0.139 ± 0.0139 b,A	0.149 ± 0.0144 ab,A
S_{mes} (m^2 m^{-2})	9.10 ± 0.53 a,A	8.93 ± 0.16 a,A	9.01 ± 0.39 a,A	11.19 ± 1.67 a,A	10.60 ± 0.28 a,B	9.66 ± 1.00 a,A
S_b area (m^2 m^{-2})	2.82 ± 0.16 a,A	2.56 ± 0.17 a,A	2.54 ± 0.14 a,A	1.89 ± 0.06 a,B	1.81 ± 0.03 a,B	1.82 ± 0.03 a,B
Interveinal distance (µm)	119 ± 3.96 a,A	142 ± 5.72 b,A	149 ± 14.18 b,A	130 ± 3.13 a,B	146 ± 2.95 b,A	141 ± 5.38 b,A

(1) Connectivity density is defined as the number of multiple connections between structures per unit volume.

References

[1] S.P. Long, X.-G. Zhu, S.L. Naidu, D.R. Ort, Can improvement in photosynthesis increase crop yields?, Plant, Cell Environ. 29 (2006) 315–330. doi:10.1111/j.1365-3040.2005.01493.x.

[2] X.-G. Zhu, S.P. Long, D.R. Ort, Improving photosynthetic efficiency for greater yield., Annu. Rev. Plant Biol. 61 (2010) 235–61. doi:10.1146/annurev-arplant-042809-112206.

[3] J.S. Amthor, From sunlight to phytomass: On the potential efficiency of converting solar radiation to phyto-energy, New Phytol. 188 (2010) 939–959. doi:10.1111/j.1469-8137.2010.03505.x.

[4] O. Ghannoum, J.R. Evans, S. von Caemmerer, Nitrogen and water use efficiency of C4 plants, in: Adv. Photosynth. Respir., Springer, 2010: pp. 129–146. doi:10.1007/978-90-481-9407-0_8.

[5] M.D. Hatch, C4 photosynthesis: a unique blend of modified biochemistry, anatomy and ultrastructure, Biochim. Biophys. Acta - Rev. Bioenerg. 895 (1987) 81–106. doi:10.1016/S0304-4173(87)80009-5.

[6] J.J.L. Pengelly, S. Kwasny, S. Bala, J.R. Evans, E. V Voznesenskaya, N.K. Koteyeva, et al., Functional analysis of corn husk photosynthesis., Plant Physiol. 156 (2011) 503–13. doi:10.1104/pp.111.176495.

[7] J.J.L. Pengelly, X.R.R. Sirault, Y. Tazoe, J.R. Evans, R.T. Furbank, S. von Caemmerer, Growth of the C4 dicot Flaveria bidentis: photosynthetic acclimation to low light through shifts in leaf anatomy and biochemistry., J. Exp. Bot. 61 (2010) 4109–22. doi:10.1093/jxb/erq226.

[8] J. Kromdijk, N. Ubierna, A.B. Cousins, H. Griffiths, Bundle-sheath leakiness in C4 photosynthesis: a careful balancing act between CO2 concentration and assimilation., J. Exp. Bot. 65 (2014) 3443–57. doi:10.1093/jxb/eru157.

[9] S. von Caemmerer, J.R. Evans, A.B. Cousins, M.R. Badger, R.T. Furbank, C4 photosynthesis and CO2 diffusion, in: J. Sheehy, P. Mitchell, B. Hardy (Eds.), Charting New Pathways to C4 Rice, International Rice Research Institute, Philippines, 2007: pp.

95–116.

[10] D. Tholen, X.-G. Zhu, The mechanistic basis of internal conductance: a theoretical analysis of mesophyll cell photosynthesis and CO2 diffusion., Plant Physiol. 156 (2011) 90–105. doi:10.1104/pp.111.172346.

[11] Q.T. Ho, H.N.C. Berghuijs, R. Watté, P. Verboven, E. Herremans, X. Yin, et al., Three-dimensional microscale modelling of CO 2 transport and light propagation in tomato leaves enlightens photosynthesis, Plant. Cell Environ. 39 (2016) 50–61. doi:10.1111/pce.12590.

[12] M. Retta, Q.T. Ho, X. Yin, P. Verboven, H.N.C. Berghuijs, P.C. Struik, et al., A two-dimensional microscale model of gas exchange during photosynthesis in maize (Zea mays L.) leaves, Plant Sci. 246 (2016) 37–51. doi:10.1016/j.plantsci.2016.02.003.

[13] R. Furbank, C. Jenkins, M. Hatch, C4 photosynthesis: Quantum requirement, C4 and overcycling and Q-Cycle involvement, Aust. J. Plant Physiol. 17 (1990) 1–7. doi:10.1071/PP9900001.

[14] R.C. Leegood, C4 photosynthesis: principles of CO2 concentration and prospects for its introduction into C3 plants, J. Exp. Bot. 53 (2002) 581–590. doi:10.1093/jexbot/53.369.581.

[15] N. Ubierna, W.E.I. Sun, D.M. Kramer, A.B. Cousins, The efficiency of C4 photosynthesis under low light conditions in Zea mays, Miscanthus x giganteus and Flaveria bidentis, Plant. Cell Environ. 36 (2013) 365–381. doi:10.1111/j.1365-3040.2012.02579.x.

[16] M.A. El-Sharkawy, Pioneering research on C4 leaf anatomical, physiological, and agronomic characteristics of tropical monocot and dicot plant species: Implications for crop water relations and productivity in comparison to C3 cropping systems, Photosynthetica. 47 (2009) 163–183. doi:10.1007/s11099-009-0030-7.

[17] N. Dengler, D. Ronald, D. Petra, H. Paul, Quantitative leaf anatomy of C3 and C4 grasses (Poaceae): Bundle sheath and mesophyll surface area relationships, Ann. Bot. 73 (1994) 241–255. doi:10.1006/anbo.1994.1029.

[18] K. Ogle, Implications of interveinal distance for quantum yield in C4 grasses: A modeling

and meta-analysis, Oecologia. 136 (2003) 532–542. doi:10.1007/s00442-003-1308-2.

[19] S. von Caemmerer, R.T. Furbank, The C4 pathway: an efficient CO2 pump., Photosynth. Res. 77 (2003) 191–207. doi:10.1023/A:1025830019591.

[20] P. Sowiński, A. Bilska, K. Barańska, J. Fronk, P. Kobus, Plasmodesmata density in vascular bundles in leaves of C4 grasses grown at different light conditions in respect to photosynthesis and photosynthate export efficiency, Environ. Exp. Bot. 61 (2007) 74–84. doi:10.1016/j.envexpbot.2007.03.002.

[21] P.W. Hattersley, Characterization of C4 type leaf anatomy in grasses (Poaceae). Mesophyll: bundle sheath area ratios, Ann. Bot. 53 (1984) 163–180. doi:http://dx.doi.org/10.1006/anbo.1994.1029.

[22] M. El-Sharkawy, J. Hesketh, Photosynthesis among species in relation to characteristics of leaf anatomy and CO2 diffusion resistance, Crop Sci. 5 (1965) 517–521. doi:10.2135/cropsci1965.0011183X000500060010x.

[23] H. Griffiths, G. Weller, L.F.M. Toy, R.J. Dennis, You're so vein: bundle sheath physiology, phylogeny and evolution in C3 and C4 plants, Plant. Cell Environ. 36 (2013) 249–261. doi:10.1111/j.1365-3040.2012.02585.x.

[24] X. Yin, Z. Sun, P.C. Struik, P.E.L. Van der Putten, W. Van Ieperen, J. Harbinson, Using a biochemical C4 photosynthesis model and combined gas exchange and chlorophyll fluorescence measurements to estimate bundle-sheath conductance of maize leaves differing in age and nitrogen content., Plant. Cell Environ. 34 (2011) 2183–99. doi:10.1111/j.1365-3040.2011.02414.x.

[25] C. Bellasio, H. Griffiths, Acclimation to low light by C4 maize: implications for bundle sheath leakiness., Plant. Cell Environ. 37 (2014) 1046–58. doi:10.1111/pce.12194.

[26] J. Kromdijk, H. Griffiths, H.E. Schepers, Can the progressive increase of C4 bundle sheath leakiness at low PFD be explained by incomplete suppression of photorespiration?, Plant. Cell Environ. 33 (2010) 1935–48. doi:10.1111/j.1365-3040.2010.02196.x.

[27] P.C. Harley, F. Loreto, G. Di Marco, T.D. Sharkey, Theoretical considerations when estimating the mesophyll conductance to CO2 flux by analysis of the response of

photosynthesis to CO2., Plant Physiol. 98 (1992) 1429–36.

[28] J.R. Evans, S. von Caemmerer, Carbon dioxide diffusion inside leaves., Plant Physiol. 110 (1996) 339–346. doi:10.1104/pp.110.2.339.

[29] X. Yin, P.C. Struik, P. Romero, J. Harbinson, J.B. Evers, P.E.L. Van Der Putten, et al., Using combined measurements of gas exchange and chlorophyll fluorescence to estimate parameters of a biochemical C3 photosynthesis model : a critical appraisal and a new integrated approach applied to leaves in a wheat (Triticum aestivum) canopy, Plant. Cell Environ. 32 (2009) 448–64. doi:10.1111/j.1365-3040.2009.01934.x.

[30] S. von Caemmerer, R.T. Furbank, Modeling C4 photosynthesis, in: R.F. Sage, R.K. Monson (Eds.), C4 Plant Biol., Academic Press, Toronto, ON, Canada, 1999: pp. 173–211.

[31] G.D. Farquhar, S. Caemmerer, J.A. Berry, A biochemical model of photosynthetic CO2 assimilation in leaves of C3 species, Planta. 149 (1980) 78–90. doi:10.1007/BF00386231.

[32] C. Bellasio, D.J. Beerling, H. Griffiths, Deriving C 4 photosynthetic parameters from combined gas exchange and chlorophyll fluorescence using an Excel tool: theory and practice, Plant. Cell Environ. (2015). doi:10.1111/pce.12626.

[33] X. Yin, D.W. Belay, P.E.L. van der Putten, P.C. Struik, Accounting for the decrease of photosystem photochemical efficiency with increasing irradiance to estimate quantum yield of leaf photosynthesis, Photosynth. Res. 122 (2014) 323–335. doi:10.1007/s11120-014-0030-8.

[34] X. Yin, P.E.L. Van Der Putten, S.M. Driever, P.C. Struik, Temperature response of bundle-sheath conductance in maize leaves, J. Exp. Bot. (2016) 1–42. doi:10.1093/jxb/erw104.

[35] O. Kiirats, P.J. Lea, V.R. Franceschi, G.E. Edwards, Bundle sheath diffusive resistance to CO2 and effectiveness of C4 photosynthesis and refixation of photorespired CO2 in a C4 cycle mutant and wild-type Amaranthus edulis., Plant Physiol. 130 (2002) 964–76. doi:10.1104/pp.008201.

[36] D. He, G.E. Edwards, Estimation of diffusive resistance of bundle sheath cells to CO2 from modeling of C4 photosynthesis, Photosynth. Res. 49 (1996) 195–208.

doi:10.1007/BF00034781.

[37] J.R. Watling, Elevated CO2 Induces Biochemical and Ultrastructural Changes in Leaves of the C4 Cereal Sorghum, Plant Physiol. 123 (2000) 1143–1152. doi:10.1104/pp.123.3.1143.

[38] Y. Zheng, M. Xu, R. Shen, S. Qiu, Effects of artificial warming on the structural, physiological, and biochemical changes of maize (Zea mays L.) leaves in northern China, Acta Physiol. Plant. 35 (2013) 2891–2904. doi:10.1007/s11738-013-1320-z.

[39] J.M. Greef, Productivity of maize (Zea mays L.) in relation to morphological and physiological characteristics under varying amounts of nitrogen supply, J. Agron. Crop Sci. 172 (1994) 317–326. doi:10.1111/j.1439-037X.1994.tb00182.x.

[40] A. Moreno-Sotomayor, A. Weiss, E.T. Paparozzi, T.J. Arkebauer, Stability of leaf anatomy and light response curves of field grown maize as a function of age and nitrogen status, J. Plant Physiol. 159 (2002) 819–826. doi:10.1078/0176-1617-00809.

[41] E. Herremans, P. Verboven, B.E. Verlinden, D. Cantre, M. Abera, M. Wevers, et al., Automatic analysis of the 3-D microstructure of fruit parenchyma tissue using X-ray micro-CT explains differences in aeration, BMC Plant Biol. 15 (2015) 264. doi:10.1186/s12870-015-0650-y.

[42] P. Verboven, O. Pedersen, E. Herremans, Q.T. Ho, B.M. Nicolaï, T.D. Colmer, et al., Root aeration via aerenchymatous phellem: three-dimensional micro-imaging and radial O2 profiles in Melilotus siculus, New Phytol. 193 (2012) 420–431. doi:10.1111/j.1469-8137.2011.03934.x.

[43] P. Verboven, E. Herremans, L. Borisjuk, L. Helfen, Q.T. Ho, H. Tschiersch, et al., Void space inside the developing seed of Brassica napus and the modelling of its function., New Phytol. 199 (2013) 936–47. doi:10.1111/nph.12342.

[44] P. Verboven, E. Herremans, L. Helfen, Q.T. Ho, M. Abera, P. Cloetens, et al., Synchrotron X-ray computed laminography of the 3-D anatomy of tomato leaves, Plant J. 81 (2015) 169–182. doi:10.1111/tpj.12701.

[45] P. Verboven, G. Kerckhofs, H.K. Mebatsion, Q.T. Ho, K. Temst, M. Wevers, et al., Three-dimensional gas exchange pathways in pome fruit characterized by synchrotron x-Ray

computed tomography, Plant Physiol. 147 (2008) 518–527. doi:10.1104/pp.108.118935.

[46] J. Flexas, M. Ribas-Carbó, A. Diaz-Espejo, J. Galmés, H. Medrano, Mesophyll conductance to CO2: current knowledge and future prospects., Plant. Cell Environ. 31 (2008) 602–21. doi:10.1111/j.1365-3040.2007.01757.x.

[47] J. Flexas, A. Díaz-Espejo, J.A. Berry, J. Cifre, J. Galmés, R. Kaldenhoff, et al., Analysis of leakage in IRGA's leaf chambers of open gas exchange systems: quantification and its effects in photosynthesis parameterization., J. Exp. Bot. 58 (2007) 1533–43. doi:10.1093/jxb/erm027.

[48] B. Genty, J.-M. Briantais, N.R. Baker, The relationship between the quantum yield of photosynthetic electron transport and quenching of chlorophyll fluorescence, Biochim. Biophys. Acta - Gen. Subj. 990 (1989) 87–92. doi:10.1016/S0304-4165(89)80016-9.

[49] V.V. Ciganda, J.S. Schepers, A. Gitelsonaj, J. Schepersc, A. Gitelson, Non-destructive determination of maize leaf and canopy chlorophyll content., J. Plant Physiol. 166 (2009) 157–67. http://www.ncbi.nlm.nih.gov/pubmed/18541334.

[50] L.A. Feldkamp, L.C. Davis, J.W. Kress, Practical cone-beam algorithm, J. Opt. Soc. Am. A. 1 (1984) 612. doi:10.1364/JOSAA.1.000612.

[51] Otsu, A threshold selection method from gray-level histograms, IEEE Trans. Syst. Man. Cybern. 9 (1979) 62–66. doi:10.1109/TSMC.1979.4310076.

[52] H.K. Mebatsion, P. Verboven, Q.T. Ho, B. Verlinden, F. Mendoza, T.A. Nguyen, et al., Modeling fruit microstructure using an ellipse tessellation algorithm, in: 13th World Congr. Food Sci. Technol., EDP Sciences, Les Ulis, France, 2006. doi:10.1051/IUFoST:20060246.

[53] J.F. Thain, Curvature correction factors in the measuremnet of cell surface areas in plant tissues, J. Exp. Bot. 34 (1983) 87–94. doi:10.1093/jxb/34.1.87.

[54] J. Evans, S. Caemmerer, B. Setchell, G. Hudson, The relationship between CO2 transfer conductance and leaf anatomy in transgenic tobacco with a reduced content of rubisco, Aust. J. Plant Physiol. 21 (1994) 475. doi:10.1071/PP9940475.

[55] J.-H. Weng, F.-H. Hsu, Gas exchange and epidermal characteristics of Miscanthus

populations in Taiwan varying with habitats and nitrogen application, Photosynthetica. 39 (2001) 35–41. doi:10.1023/A:1012483600367.

[56] S.D. Loriaux, T.J. Avenson, J.M. Welles, D.K. Mcdermitt, R.D. Eckles, B. Reinsche, et al., Closing in on maximum yield of chlorophyll fluorescence using a single multiphase flash of sub-saturating intensity, Plant. Cell Environ. 36 (2013) 1755–1770. doi:10.1111/pce.12115.

[57] R.F. Sage, R.K. Monson, S. von Caemmerer, R.T. Furbank, Modeling C4 Photosynthesis, in: C4 Plant Biol., 1999: pp. 173–211.

[58] X. Yin, P.C. Struik, Mathematical review of the energy transduction stoichiometries of C4 leaf photosynthesis under limiting light., Plant. Cell Environ. 35 (2012) 1299–312. doi:10.1111/j.1365-3040.2012.02490.x.

[59] J. Galmés, J.M. Ochogavía, J. Gago, E.J. Roldán, J. Cifre, M.À. Conesa, Leaf responses to drought stress in Mediterranean accessions of Solanum lycopersicum: Anatomical adaptations in relation to gas exchange parameters, Plant, Cell Environ. 36 (2013) 920–935. doi:10.1111/pce.12022.

[60] C.L.D. Jenkins, R.T. Furbank, M.D. Hatch, Inorganic carbon diffusion between C4 mesophyll and bundle sheath cells: Direct bundle sheath CO2 assimilation in intact leaves in the presence of an inhibitor of the C4 pathway., Plant Physiol. 91 (1989) 1356–63. doi:10.1104/pp.91.4.1356.

[61] R.H. Brown, G.T. Byrd, Estimation of bundle sheath cell conductance in C4 species and O2 insensitivity of photosynthesis., Plant Physiol. 103 (1993) 1183–1188. doi:10.1104/pp.103.4.1183.

[62] M.M. Barbour, J.R. Evans, K.A. Simonin, S. von Caemmerer, Online CO 2 and H 2 O oxygen isotope fractionation allows estimation of mesophyll conductance in C 4 plants, and reveals that mesophyll conductance decreases as leaves age in both C 4 and C 3 plants, New Phytol. 59 (2016). doi:10.1111/nph.13830.

[63] P. Rezvani Moghaddam, D. Wiliman, Cell wall thickness and cell dimensions in plant parts of eight forage species, J. Agric. Sci. 131 (1998) 59–67. doi:10.1017/S0021859698005632.

[64] P.W. Hattersley, A.J. Browning, Occurrence of the suberized lamella in leaves of grasses of different photosynthetic types. I. In parenchymatous bundle sheaths and PCR ("Kranz") sheaths, Protoplasma. 109 (1981) 371–401. doi:10.1007/BF01287454.

[65] P. Sowiński, J. Szczepanik, P.E.H. Minchin, On the mechanism of C4 photosynthesis intermediate exchange between Kranz mesophyll and bundle sheath cells in grasses., J. Exp. Bot. 59 (2008) 1137–47. doi:10.1093/jxb/ern054.

[66] N.G. Dengler, T. Nelson, Leaf structure and development in C4 plants, in: R.F. Sage, R.K. Monson (Eds.), C4 Plant Biol., Academic Press, Toronto, ON, Canada, 1999: pp. 133–172.

[67] R.A. Mertz, T.P. Brutnell, Bundle sheath suberization in grass leaves: multiple barriers to characterization., J. Exp. Bot. 65 (2014) 3371–3380. doi:10.1093/jxb/eru108.

[68] P. Sowiński, A. Rudzińska-Langwald, P. Kobus, Changes in plasmodesmata frequency in vascular bundles of maize seedling leaf induced by growth at sub-optimal temperatures in relation to photosynthesis and assimilate export, Environ. Exp. Bot. 50 (2003) 183–196. doi:10.1016/S0098-8472(03)00021-2.

[69] D.F. Parkhurst, K. a Mott, Intercellular diffusion limits to CO2 uptake in leaves : Studies in Air and Helox., Plant Physiol. 94 (1990) 1024–32. doi:10.1104/pp.94.3.1024.

[70] X.P. Feng, Y. Chen, Y.H. Qi, C.-L. YU, B.-S. Zheng, M. Brancourt-Hulmel, et al., Nitrogen enhanced photosynthesis of Miscanthus by increasing stomatal conductance and phosphoenolpyruvate carboxylase concentration, Photosynthetica. 50 (2012) 577–586. doi:10.1007/s11099-012-0061-3.

[71] Y. Tazoe, K. Noguchi, I. Terashima, Effects of growth light and nitrogen nutrition on the organization of the photosynthetic apparatus in leaves of a C4 plant, Amaranthus cruentus, Plant, Cell Environ. 29 (2006) 691–700. doi:10.1111/j.1365-3040.2005.01453.x.

[72] J. Vos, P.E.L. van der Putten, C.J. Birch, Effect of nitrogen supply on leaf appearance, leaf growth, leaf nitrogen economy and photosynthetic capacity in maize (Zea mays L.), F. Crop. Res. 93 (2005) 64–73. doi:10.1016/j.fcr.2004.09.013.

[73] H. Poorter, U. Niinemets, L. Poorter, I.J. Wright, R. Villar, Causes and consequences of variation in leaf mass per area (LMA):a meta-analysis, New Phytol. 182 (2009) 565–588.

doi:10.1111/j.1469-8137.2009.02830.x.

[74] Y. Wang, S.P. Long, X.-G. Zhu, Elements required for an efficient NADP-malic enzyme type C4 photosynthesis., Plant Physiol. 164 (2014) 2231–46. doi:10.1104/pp.113.230284.

[75] R.F. Sage, A.D. McKown, Is C4 photosynthesis less phenotypically plastic than C3 photosynthesis?, J. Exp. Bot. 57 (2005) 303–317. doi:10.1093/jxb/erj040.

[76] E. Utsunomiya, S. Muto, Carbonic anhydrase in the plasma membranes from leaves of C3 and C4 plants, Physiol. Plant. 88 (1993) 413–419. doi:10.1034/j.1399-3054.1993.880304.x.

[77] C. Maurel, L. Verdoucq, D.-T. Luu, V. Santoni, Plant aquaporins: membrane channels with multiple integrated functions, Annu. Rev. Plant Biol. 59 (2008) 595–624. doi:10.1146/annurev.arplant.59.032607.092734.

Response to reviewer

Reviewer #1:

The manuscript "Impact of anatomical traits of maize ……" describes the changes in the bundle sheath conductance and also the related changes in the anatomical features in both nitrogen and age treatments. The data presented are very comprehensive and informative. There are a number of issues that need to be clarified.

The procedure for fitting the GE and CF curves are not clear from the current writing. It is understood that the estimation was conducted using a code that was published earlier. However, are all the assumptions in the original code appropriate for the current study? By reading the earlier paper Yin *et al*. (2011) on estimating parameters of C_4 photosynthesis model, it is assumed that 10 % of the PSII activity are partitioned into the bundle sheath cells. It is important to test how this assumption would influence the estimate of bundle sheath conductance and leakiness if this assumption is biased. A sensitivity analysis is therefore recommended for this.

RESPONSE: we did not conduct this sensitivity analysis with respect to α in the present paper when we submitted because this was done by Yin *et al*. (2011) who showed that the estimated g_{bs} was virtually insensitive when α was varied from 0 to 0.45. That study also did a sensitivity analysis with respect to a number of other input parameters which we list here with their default values in the Table 1 (below). In addition, comment (2) from the reviewer required a sensitivity analysis with respect to parameter *x*, which is also in the Table 1.

To respond to this reviewer's comments 1 and 2, we carried out a full set of sensitivity analysis, and the results are shown in Fig. 1 and Table 2 below.

Table 1. Lists of model parameters used both in the model presented in the current manuscript and in the method of Yin *et al*. (2011).

Symbols	Definitions	Values	References
K_p	Michaelis-Menten constant of PEPC for CO_2	40 µbar	(Pfeffer and Peisker, 1998)
$K_{m,c}$	Michaelis-Menten constant of Rubisco for CO_2	485 µbar	(Cousins et al., 2010)
$K_{m,O}$	Michaelis-Menten constant of Rubisco for O_2	146 mbar	(Cousins et al., 2010)
$S_{c/o}$	Relative CO_2/O_2 specificity factor for Rubisco	2826 (-)	(Cousins et al., 2010)
α	Fraction of Photosystem II activity in bundle sheath	0.1	(von Caemmerer and Furbank, 1999)
x	Partitioning factor of J_{ATP} to the C_4 cycle	0.4	(von Caemmerer and Furbank, 1999)

Table 1 shows that many of the assumed parameters are enzyme properties, which could be expected to vary less within species compared to maximum catalytic activities of the enzymes. It should be noted that due to the assumption of light-limited assimilation in our model formulation, enzyme properties are less likely to influence our estimation. However, for clarity we show the sensitivity in Fig. 1. The estimates were g_{bs}, the lumped calibration factor (s') and, the slope of linearity between mesophyll conductance (X_{gm}) and leaf nitrogen content. The sensitivity analysis was carried out by considering the following changes; 0.25, 0.50, 1.25 and 1.50 times the default value listed in Table 1.

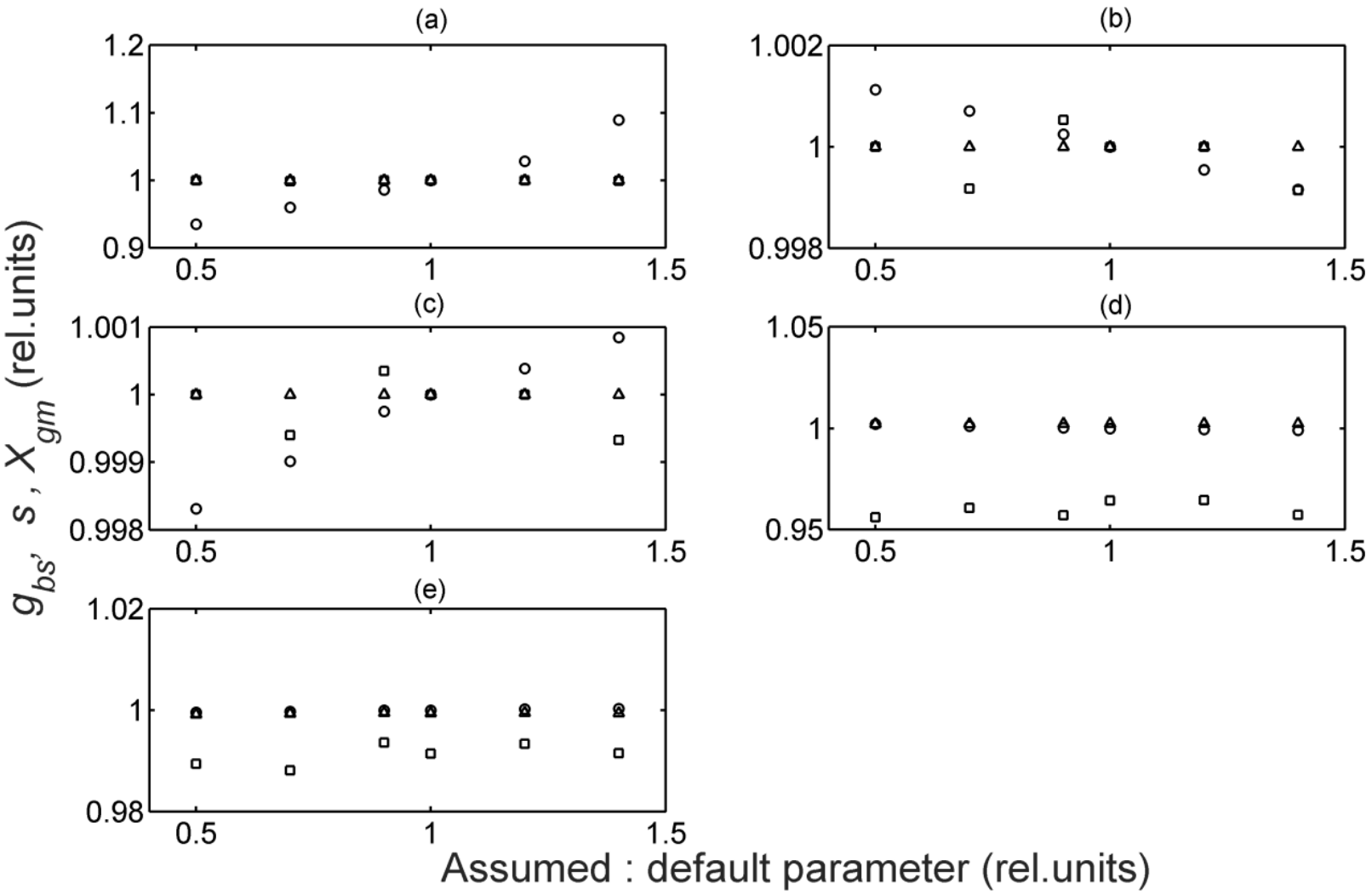

Figure 1. Sensitivity of the estimated values of g_{bs} (square), s' (triangle) and X_{gm} (circle) to input parameters such as K_p (a), $K_{m,C}$, (b) $K_{m,O}$, (c) $S_{c/o}$, (d) and α (e). The changes in the estimated parameters were expressed by dividing the new parameter by the default value given in Table 1 (here). The parameters g_{bs} and s' were an average of the estimates for all leaf types corresponding to each change in the input parameters.

Fig. 1 shows that the estimated g_{bs}, s' and X_{gm} were not sensitive to input parameters listed in Table 1 including the fraction of PSII in bundle sheath cells (α), confirming the result of Yin *et al*. (2011).

Table 2 shows that X_{gm} and s' were largely insensitive to various values of x except when it is low (0.35). However, the value x = 0.35 may not be biologically realistic as many modeling studies show that x is very close 0.40 (von Caemmerer and Furbank, 1999; Yin et al., 2011) under various treatment and ambient conditions. Yin & Struik (2012) estimated that when additional ATP utilizing processes were considered, x varies from 0.399 to 0.385. Optimization analysis showed that the optimum x stayed ca. 0.4 over a wide range of conditions, only except under extremely low light condition (von Caemmerer and Furbank, 1999). When x was also estimated simultaneously with g_{bs} from our model, it was 0.43 ± 0.042 which is also close to 0.4. We chose to fix x = 0.4 to improve the estimation of g_{bs} by reducing the number of parameters that should be fitted simultaneously.

Table 2 shows that the estimated values of g_{bs} were highly sensitive to assumptions regarding the values of x expectedly due to the assumption of light-limited photosynthesis rate. Due to the high standard error in some of the estimated g_{bs} (Fig. 4 of manuscript and Fig. 2 here) we are not certain about the actual values of them as was also discussed in the current manuscript. However, Fig. 2 shows that the relationship between g_{bs} and leaf nitrogen content (LNC) remained strongly linear. Therefore, although the estimated bundle sheath conductances were sensitive to the choice of x, the relationship between g_{bs} and LNC was minimally affected. This is in line with our main intention in current manuscript.

In the revised manuscript, we now added a new section (section 3.4) on lines 283-302 to discuss the sensitivity of g_{bs} to x. Table 2 and Fig. 2 were included in supplementary materials as Table S4 and Fig. S4 respectively. For completeness, the lack of sensitivity g_{bs} to the other parameters in Table 1 which was the result of our assumption is shown in Fig. S10 (supplementary materials).

Table 2. Sensitivity of parameters, slope of linearity between mesophyll conductance and leaf nitrogen content (Xg_m), lumped calibration factor (s') and bundle sheath conductance (g_{bs}) for assumed values of the fraction of ATP allocated to the C_4 cycle (x). The leaf nitrogen (N) contents are represented by low (N1), intermediate (N2) and high (N3) for young (A1), and old (A2) leaves.

		$s'/s'_{x=0.4}$						$g_{bs}/g_{bs\ x=0.4}$					
x	Xg_m	N1A1	N1A2	N2A1	N2A2	N3A1	N3A2	N1A1	N1A2	N2A1	N2A2	N3A1	N3A2
0.35	1.00	1.16	1.14	1.14	1.14	1.14	1.15	1.47	0.93	0.77	0.73	0.77	0.77
0.40	1.00	1.00	1.00	1.00	1.00	1.00	1.00	1.00	1.00	1.00	1.00	1.00	1.00
0.45	1.01	0.98	0.99	0.99	0.99	0.99	0.99	2.19	2.82	2.29	3.07	2.40	2.40
0.50	1.02	0.98	0.99	0.98	0.99	0.98	0.98	3.59	4.99	3.81	5.61	4.25	3.95

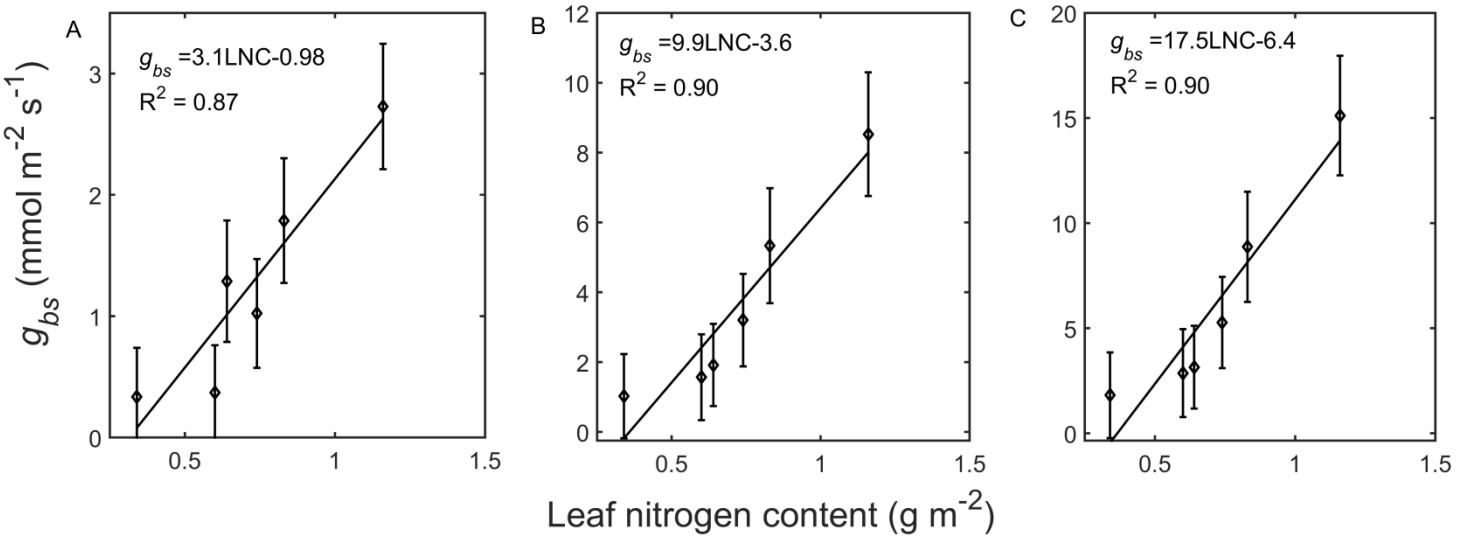

Figure 2. Relationship between bundle sheath conductance (g_{bs}) and leaf nitrogen content (LNC) for various fractions of ATP partitioned to C_4 cycle (x): x = 0.35 (panel A), x = 0.45 (panel B) and x = 0.50 (panel C). Bar represent standard error (n=4).

2. Similarly, a value of 0.4 was used to partition the amount of ATP to C4 cycle as well. Some recent evidence suggests that under different conditions, the Rubisco and PEPC activities change and the ratio between them can alter. As a result, the proportion of energy portioned into the C3 cycle and the C4 cycle might change under different treatments. Some sensitivity analysis will be desired to test their influence on the estimated conductance and leakiness.

RESPONSE: sensitivity of the g_{bs}, X_{gm} and s' to x is already addressed in the response to the comment 1 (above). Below, we present the sensitivity of the estimated leakiness to x.

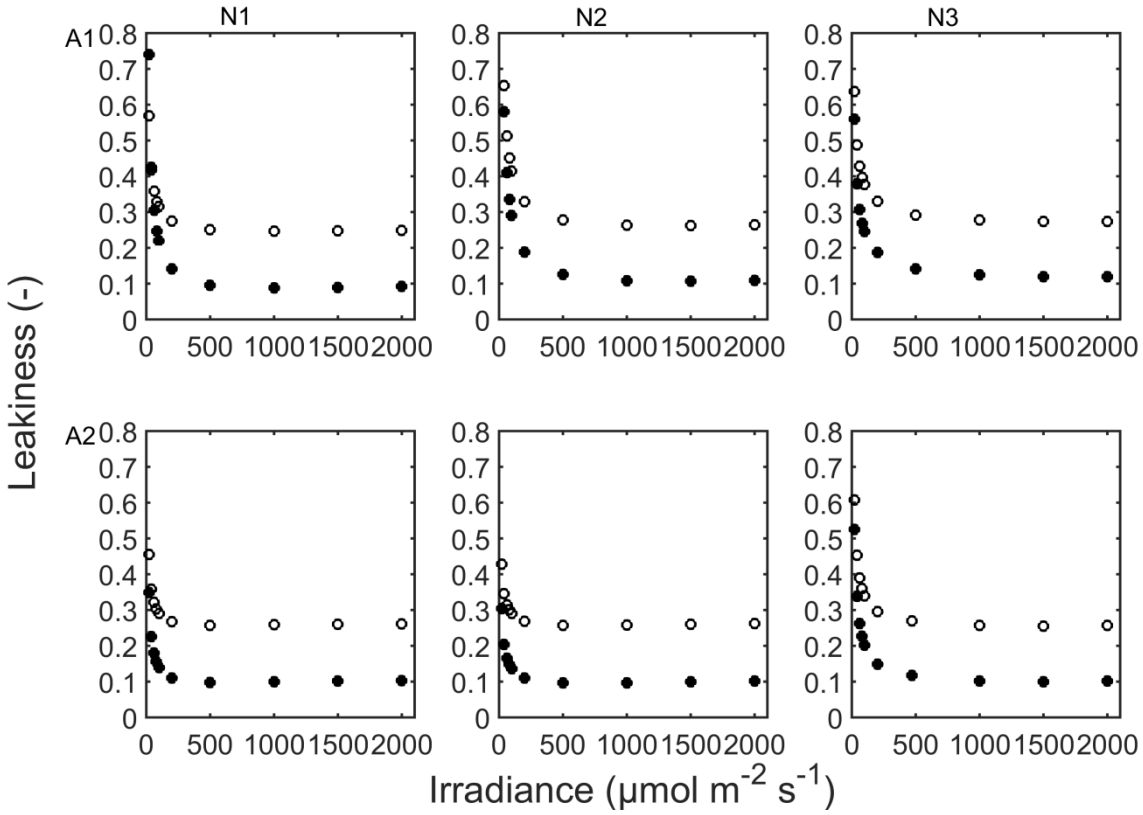

Figure 3. Sensitivity of estimated leakiness in response to irradiance for fraction of ATP allocated to the C_4 cycle (x): x = 0.4 (filled circles) and x = 0.45 (open circles). Leaf types were: young (A1) and old (A2) leaves from maize plant grown under low (N1), intermediate (N2) and high (N3) nitrogen supply. The oxygen concentration was 21 %.

Fig. 3 shows that the estimated leakiness was sensitive to x due to 2 to 3 times higher g_{bs} (Table 2 above). In addition, similar to our previous results (filled circles in Fig. 3, here), leakiness was largely similar among the leaf types. Therefore, we added a brief description on lines 298-300

stating the sensitivity of the predicted leakiness and the mean concentration of CO_2 in bundle sheath cells to *x*. Fig. 3 was also included in supplementary materials as Fig. S8 (supplementary materials) and the response of the mean concentration of CO_2 in bundle sheath cells was added to supplementary materials as Fig. S9.

In conclusion, changing the value of *x* does not affect the strong linear relationship between g_{bs} and LNC, which is the main focus of our study. Although the prediction of leakiness was also sensitive to the exact value of *x*, the stability of leakiness across treatments as was also highlighted in the manuscript did not change. Moreover, prediction of leakiness was not our main intention in the current manuscript and the predictions should be considered only temporary.

3. Lines 218-222. It is difficult to understand how would a maize leaf being constantly light limited under different light and CO2 levels. The relationship between quantum efficiency of CO2 fixation and that of the PSII electron transfer should not be used as an argument that the system is constantly limited by electron transfer as well. Limitation in the enzyme activity would feedback to decrease the CO2 fixation rate, which can also in principle generate a good relationship between electron transport and CO2 fixation. The linear relationship suggests that the proportion of ATP or energy used for sinks other than CO2 fixation was not altered during the measurements.

RESPONSE: we agree with this reviewer that the linear relationship suggests that the proportion of ATP or energy used for sinks other than CO_2 fixation was not altered during the measurements so that any enzymatic limitation, if occurred, had a feedback effect on electron transport.

A strong linear relationship between quantum efficiency of CO_2 fixation and that of PSII electron transport has been reported for various C_4 plants, including maize (Krall and Edwards, 1990). In particular, Krall and Edwards (1990) observed such a close coupling even under very low intercellular CO_2 in the range of 40 – 50 µbar. They interpreted this as C_4 plants still using a large amount of light energy in photosynthesis even under low CO_2. In addition, limitation of photosynthesis, mainly by electron transport was also observed in our previous measurement for maize leaves (Yin et al., 2011). At the time of the measurement, we could measure only a few physiological parameters such as rate of photosynthesis, intercellular CO_2 and quantum efficiency of PSII electron transport. We agree that this must be carefully interpreted as several factors such as feedback regulation and possible co-limitation might also play a role. However, this could be resolved when enzyme activity measurements are also done.

In the manuscript, line 218-223 we corrected the interpretation of the linear relationship between the quantum efficiency of CO_2 fixation and that of PSII electron transport.

4. Following the above point. Some good explanation is needed to elucidate why unrealistic estimation of the Vcamx and Vpamx was obtained.

RESPONSE: In the manuscript, lines 223-226 we added explanations for why unrealistic estimates of $V_{c,max}$ and $V_{p,max}$ were obtained.

5. The code used for parameter fitting is not in open source, hence it is difficult to evaluate the potential parameter assumptions used in fitting the GE and CF data. It would be important to list out all the parameters used in the curve fitting to enable later replication of the work.

RESPONSE: Yin *et al.* (2011) indicated in their article that the code could be obtained upon request, so the code is open. In fact, Dr Yin (a coauthor of the present manuscript) has already received many requests, and he has sent the code to the requesters. This is also indicated on line 213 of the present manuscript.

A full list of parameters was given in supplementary material Table S1 (supplementary materials).

References

von Caemmerer, S. and Furbank, R.T. (1999). Modeling C4 photosynthesis. In C4 plant biology, R.F. Sage and R.K. Monson, eds (Academic Press: Toronto, ON, Canada), pp. 173–211.

Cousins, A.B., Ghannoum, O., von Caemmerer, S., and Badger, M.R. (2010). Simultaneous determination of Rubisco carboxylase and oxygenase kinetic parameters in Triticum aestivum and Zea mays using membrane inlet mass spectrometry. Plant. Cell Environ. **33**: 444–452.

Krall, J.P. and Edwards, G.E. (1990). Quantum yields of photosystem II electron transport and carbon dioxide fixation in C4 plants. Aust. J. Plant Physiol. **17**: 579–88.

Pfeffer, M. and Peisker, M. (1998). CO2 gas exchange and phosphoenolpyruvate carboxylase activity in leaves of Zea mays L. Photosynth. Res. **58**: 281–291.

Yin, X. and Struik, P.C. (2012). Mathematical review of the energy transduction stoichiometries of C4 leaf photosynthesis under limiting light. Plant. Cell Environ. **35**: 1299–312.

Yin, X., Sun, Z., Struik, P.C., Van der Putten, P.E.L., Van Ieperen, W., and Harbinson, J. (2011). Using a biochemical C4 photosynthesis model and combined gas exchange and chlorophyll fluorescence measurements to estimate bundle-sheath conductance of maize leaves differing in age and nitrogen content. Plant. Cell Environ. **34**: 2183–99.

Supplementary Interactive Plot Data (CSV)

Click here to download Supplementary Interactive Plot Data (CSV): Supplementary materials.docx

Highlights

- Bundle sheath conductance positively correlated with leaf nitrogen content.
- Bundle sheath conductance impacted by leaf nitrogen content related little with anatomy.
- Combined effect of leaf nitrogen content and age on anatomy caused variations of bundle sheath conductance.